Article
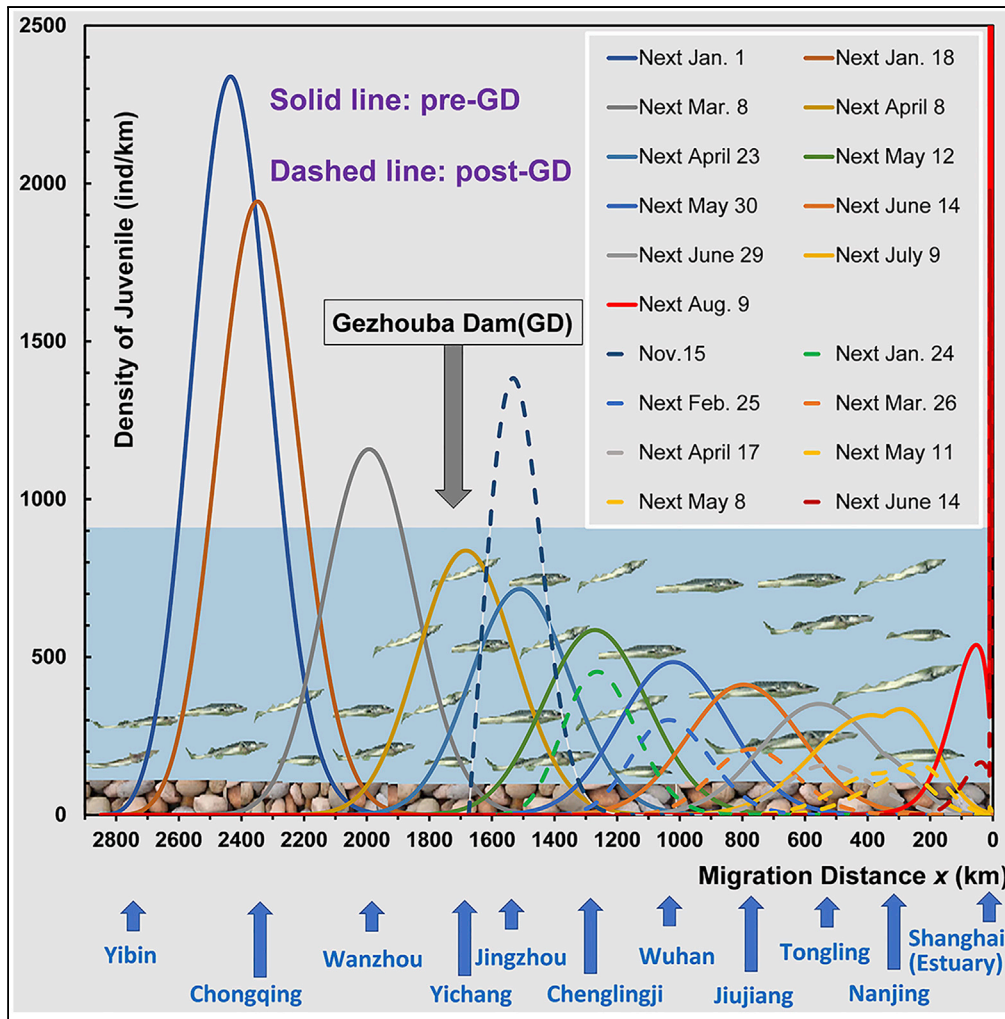
Drifting with Flow versus Self-Migrating—How Do Young Anadromous Fish Move to the Sea?

Zhenli Huang

zhlhuang@263.net

HIGHLIGHTS

The migration process of young fish depends on their age and the local water flow

Weak swing or swimming of larvae plays a crucial role in fish survival in the river

Young fish move in a gradually transforming manner—passive drift to active swimming

The Dam causes juveniles to reach the estuary earlier, which pose a mortality risk

Article

Drifting with Flow versus Self-Migrating—How Do Young Anadromous Fish Move to the Sea?

Zhenli Huang[1,2,*]

SUMMARY

The downriver migration process of young anadromous fish has a far-reaching impact on their survival rate and the efficacy of hatchery-reared fish release, but it is poorly understood. Moreover, the impact of dams on the fish remains unclear. The Chinese sturgeon is an anadromous and dam-affected fish in the Yangtze River. Here, we propose a novel theoretical framework to reveal the migration process of young Chinese sturgeon. We clarify the effects of active swimming of fish and water flow on the downriver migration and the parametric traits of the migrational stages. Then, we show that the young fish migrate downriver along the inshore waters in a gradually transforming manner from passive drift to active swimming. Lastly, we evaluate the impact of the Gezhouba Dam (GD) on the migration of the young fish, as well as demonstrate the life cycles of Chinese sturgeon in the Yangtze River pre- and post-GD.

INTRODUCTION

Understanding the mechanisms driving an aquatic organism's movement is an essential component in the conservation and management of species and ecosystems. The migration pattern of aquatic organisms plays a fundamental role in the survival of their populations, especially for migratory fish, which usually depend on their swimming ability and the towing capacity of the water flow or both. In the past, water flow was presumed to dominate organisms' movements. However, at present there is a consensus that active swimming, even at seemingly trivial speeds, could have profound consequences for the movements, fitness, and distribution of marine organisms (Fossette et al., 2015; Putman and Mansfield, 2015; Putman et al., 2016). The situation for river organisms, especially anadromous fish, remains poorly understood.

The anadromous fishes, comprising 110 species that live in seas and migrate into fresh water to spawn, play a significant role in linking the river-sea ecosystem (Kynard et al., 2002; Braaten et al., 2008, 2012; Stoll and Beeck, 2012; Huang and Wang, 2018). The downriver migration process of young fish has far-reaching impacts on the survival of fish and the efficacy of hatchery-reared fish release. There is minimal and fragmentary information concerning local river reach (Braaten et al., 2008, 2012) mainly due to technical obstacles in sampling, identifying individual ages, tracking the fish (Braaten and Fuller, 2007), and the fact that there is no robust theoretical model. Larvae or juveniles are assumed to act as passive bodies, traveling with the river's flow; however, this method underestimates the weak active swimming ability of young fish (YARSG, 1988; Auer and Baker, 2002; Stoll and Beeck, 2012). Moreover, dams are regarded as a serious threat to anadromous fish, and the mechanism by which dams affect the young fish remains unclear.

Fisheries restocking programs have primarily been applied to bolster stocks by rearing fish in hatcheries and releasing them into the wild. This is at a time when the world's fish species are under threat from habitat degradation and over-exploitation. However, the behavioral deficits displayed by hatchery-reared fish and the resulting poor survival rates in the wild have been noted for over a century (Brown and Day, 2002). In China, artificial restocking of fish and release has been used as the sole remedial measure of dam construction for rescuing rare and endangered fish, and its efficacy has been controversial. Brown and Day (2002) emphasized that the focus of fisheries research must shift from husbandry to improving post-release behavioral performance. Thus, how to assess and improve post-release performance of cultured fish is closely related to a fundamental issue: detailing the migration process of juveniles in the river.

Chinese sturgeon (*Acipenser sinensis*) is a typical example of the 16 species of anadromous sturgeon globally and is a flagship species of the Yangtze River. The sturgeon was listed as critically endangered by the International Union for Conservation of Nature (IUCN) in 2010 and included in Appendix II of Convention on

[1]China Institute of Water Resources and Hydropower Research, Beijing 100038, China

[2]Lead Contact

*Correspondence: zhlhuang@263.net

International Trade in Endangered Species of Wild Fauna and Flora (CITES) in 2015. Before the river closure by the Gezhouba Dam (GD), the crucial first and lowermost water project on the Yangtze River on 4 January 1981 (pre-GD), spawning Chinese sturgeons spread in the 800-km reach between Maoshui (Yibin City, Sichuan Province) and Wanzhou (Chongqing Municipality) and spawned at 19 sites. The Chinese sturgeon enters the Yangtze River between June and August every year when the gonadal development of the adult fish reaches stage III (males, 8 years old; females, 13 years or older) while fasting all along the way and migrating 2,850 km to the upstream spawning ground. After breeding in autumn of the following year, 15 months after initially entering the Yangtze River, the adult fish returns to the sea within 1 month (Huang and Wang, 2018). Hatched larvae begin to migrate downriver in October or November each year and reach the estuary in the next summer, all the while foraging along the way and adapting to the saltwater environment of estuarine areas such as the eastern beach of Chongming Island. After 1981 (post-GD), the spawners were forced to lay eggs in a less suitable spawning ground about 30 km downstream of the GD (Figures 1A and 1B). However, with the operation of the cascade dams on the upper reaches of the Yangtze River, especially the Three Gorges and Xiluodu dams, the population of Chinese sturgeon has continually decreased to the verge of extinction (Wu et al., 2015).

Before the 1990s, there was insufficient information concerning the population migration or dynamics of Chinese sturgeon except for fishing or bycatch records (YARSG, 1988). Since then, biotelemetry, hydroacoustic detection, and mark-recapture techniques have been widely used in the study of the Chinese sturgeon (Kynard et al., 1995; Yang et al., 2005; Lin, 2008; Wang et al., 2012, 2014). Only the mark-recapture technique can be used to obtain the interval speed between the releasing place to the recapture site of larvae or juveniles, because their body sizes are too small to be monitored (tracked or detected) by biotelemetry or hydroacoustic detection (Yang et al., 2005; Wang et al., 2014). Therefore, we cannot clarify the mechanism of the downriver migration for larvae or juveniles with existing technology. Taking the Chinese sturgeon as a model organism, Huang and Wang (2018) proposed the Migration Dynamics Model (MDM) for anadromous or dam-affected fish and successfully applied it to the spawning upriver and post-spawning downriver migration processes of adult Chinese sturgeon in the Yangtze River. Theoretically, this model can be used for young fish, but juveniles have more complicated behavior than adults, such as avoiding predation and feeding; this is related to ontogenetic behavior and the hydrodynamic impacts. Here we attempt to establish a novel framework for theoretical modeling to analyze the downriver migration process of young Chinese sturgeon and to evaluate the impact of the dams on the migration process.

We used the number of days post-hatching (dph) to characterize the age of the fish rather than the number of days after fertilization. The early life stages of the fish vary greatly in morphology and physiology and are usually divided into three developmental stages, namely: early larva (0–11 dph), late larva (12–39 dph), and juvenile (40 + dph) (Zhuang, 1999; Zhuang et al., 2002). The juveniles more than 40 dph old have external characteristics like the adult fish. Here we also used an overall term, young fish, to refer to these fish at all developmental stages from the hatching site to the estuary, and we set up a coordinate system by taking the Yangtze mouth as the origin point and tracing upriver (Figure 1A).

RESULTS

Considering the mortality of young fish along the migratory path, we derived a modified Migration Dynamics Model (MDM) for the young fish. The key to solving the MDM is to estimate the following three parameters: the migration velocity (U), the diffusion coefficient (D), and the mortality rate (K). Of these, U and D are directed toward the fish as a living body, rather than a passive body (Stoll and Beeck, 2012). Previous studies considered only the speed of the water flow and neglected the swimming ability of the larvae (Erwin and Jacobson, 2015). The swimming ability of the larvae increases with age, whereas the effect of the current on U and D diminishes. Therefore, we considered that the migration speed and the diffusion coefficient of juveniles depend on both the age of the larvae and the water flow. According to the ontogenetic development and ecological behavior of the fish, we divided the downriver migration process into three phases: drift stage, cover stage, and self-migration stage (Figure 2). Of the three, the last stage is predominant in length and time. Based on the river zoning and including the effects of riverbanks and tides on the migration of young fish, we built formulas of divided functions on the three parameters at each stage and then calculated the migration processes of young fish by numerical methods (see Transparent Methods).

Migration Stage Division and Its Distinguishing Features

(1) Drift stage (0–8 dph): This stage involves mainly the downstream area of the spawning ground. The spawners lay eggs that adhere to the rocks at the bottom of the spawning ground, attracting predators. Five days later, the
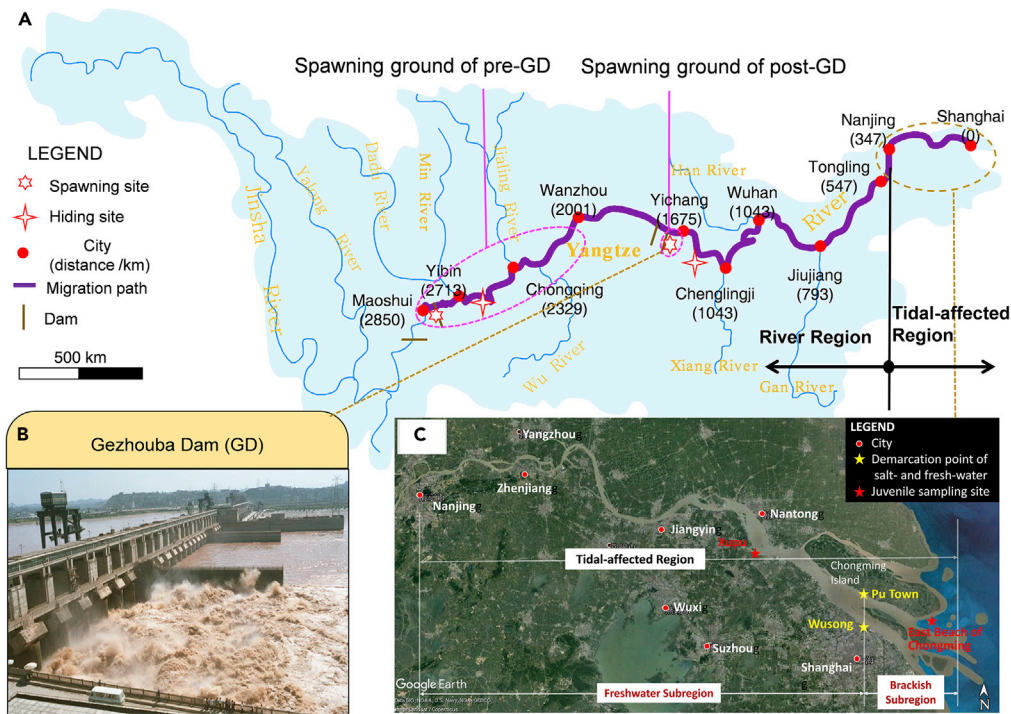
Figure 1. Zoning of Migration Path and Spawning Grounds of Chinese Sturgeon Pre- and Post-GD

(A) The Yangtze River basin showing spawning grounds pre- and post-GD and the migration zoning of the juveniles. Here, the bold purple line indicates the migration path of the Chinese sturgeon. River kilometers (km) are used as the unit of distance, days (d) as the unit of time, and number of individuals (ind) as fish quantity. The navigation channel mileage was used to calculate the coordinates of the main cities along the river. Numbers in parentheses below city ports are river distances from the Yangtze mouth (km).

(B) The GD is the first and the lowest dam built on the main stem of the Yangtze River. After 1981 (post-GD), the spawners had to lay eggs in a less suitable spawning ground about 30 km downstream of the GD.

(C) The tidal-affected region below Nanjing consists of freshwater and brackish subregions, demarcated at Wusong or Pu Town indicated by yellow stars. The red stars at Xupu and the eastern beach of Chongming Island indicate the sampling sites of juveniles in the estuarine area. According to estuarine salinity, the tidal-affected region can be further divided into freshwater and brackish subregions. The saltwater intrusion caused by tidal current affects not only the flow velocity but also the salinity. The range of the brackish subregion depends on the interaction between the Yangtze River runoff and the salt tide, near the mouth of the estuary. North and south branches bifurcate the estuary of the Yangtze River. The south is the mainstream area, but the salt tide invades the north with high salinity. In the dry season, the saltwater of the north flows backward and invades the south from the bifurcation point. Therefore, we consider the south branch as the migration path of juveniles from May to August of each year instead of the north branch, which was confirmed by an investigation between 1982 and 1993 showing no juvenile Chinese sturgeon in the north branch (Yi, 1994). Bao and Zhu (2017) calculated the horizontal and vertical salinity distribution of the estuary during the spring tide and the low tide in the 1950s and the 1970s, and in 2012. They concluded that, according to the drinking water salinity standard of 0.45 psu, the upper boundary of saltwater intrusion in the south branch is near Wusong and Pu Town, about 30 km from the East Beach of Chongming Island. However, salinity had less effect on the swimming ability of juveniles over 7 months of age (He et al., 2013).

See also Figure S1.

fertilized eggs hatch and start to move downstream with the water current; the early larvae survive through endogenous nutrition and do not forage. Figure S1A shows the velocity vector of the early larvae, longitudinally drifting with the current, while laterally swimming to shores, as well as vertically going up to the water surface or down to the riverbed (Figure 2A). The longitudinal U of larvae mainly depends on the uneven velocity distribution of the current at different water layers where the larvae stay (Figure 2B). The larvae gradually go up to the surface and then down to the bottom (Figure 2C). Therefore, the drift velocity of the larvae depends on the spatial position of the river cross-section. When they drift longitudinally with the current, the larvae move horizontally to shallow waters near the shore through a weak swing due to their phototaxis. The larvae prefer shallow water for survival and future feeding. Hence, the riverbank has a significant effect on the speed of larval movement.
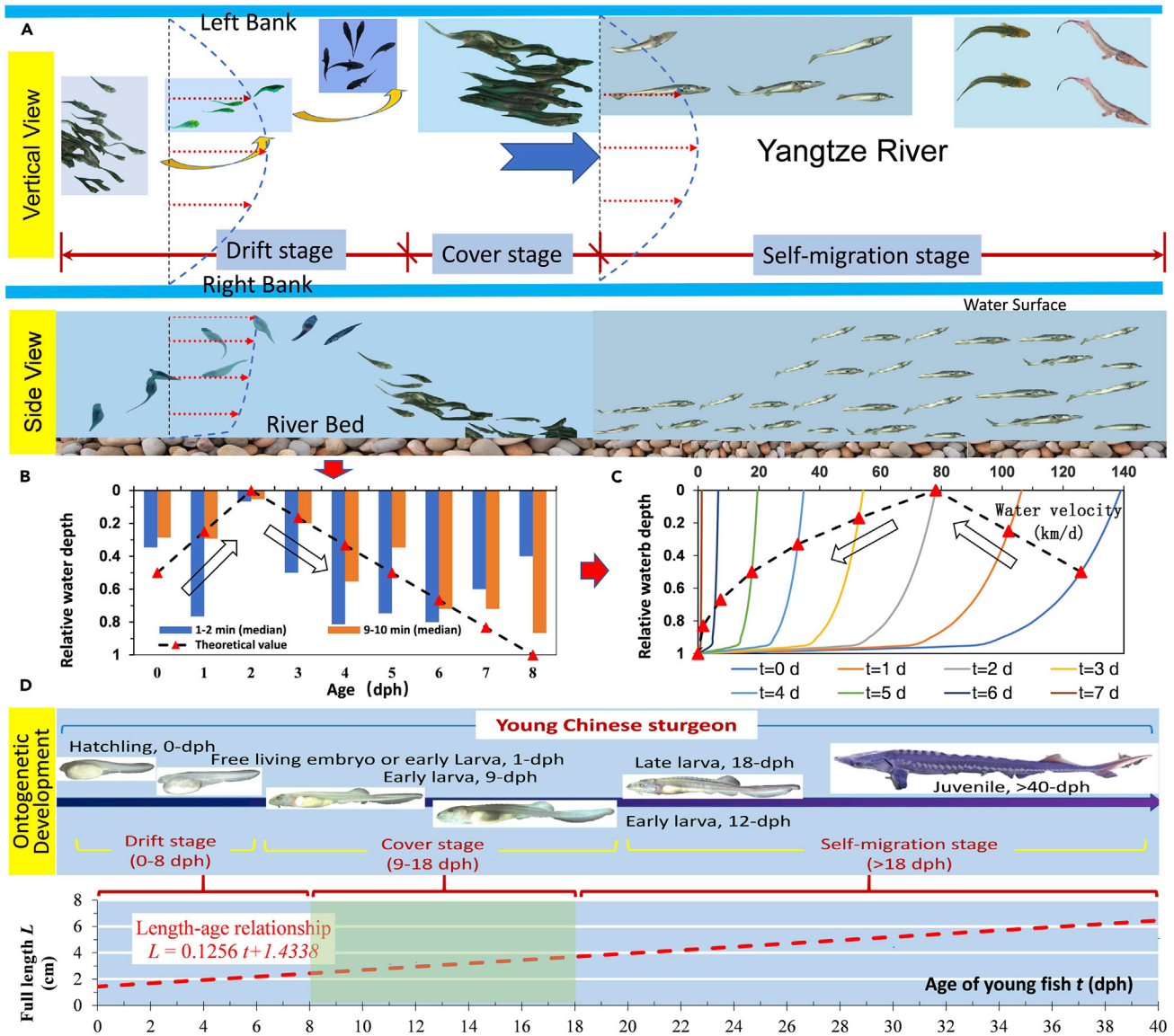
Figure 2. Schematic Diagram of the Downriver Migration Process of Young Chinese Sturgeon

(A) The vertical (top) and side (bottom) views of the young fish migration path in the Yangtze River. Here we assume the Yangtze River as an open channel. The dotted lines represent the lateral (top) and vertical (bottom) velocity distributions of the current. The elevation view shows that, in the drift stage, the free-living embryos or early larvae migrate from the middle of the river to both shores while they are moving downward after hatching, and then enter the cover stage during which the early larvae hide on the inshore bottom of the river bed. After 18 dph, the late larvae enter the self-migration stage and then migrate downstream along the inshore waters. The side view shows that the juveniles move vertically to the water surface at 1–2 dph of age while drifting with the current and then move to the riverbed at 3–7 dph until at 8–18 dph when they enter the cracks of riverbed substrate for hiding and avoiding predation. After 18 dph of age, the juveniles migrate downstream, depending on their swimming ability; they are also affected by the current.

(B) The location of the water layer (relative water depth) of the early larvae at different ages (dph) during the drift stage. According to the water depth preference of early larvae (Zhuang, 1999; Zhuang et al., 2002), we assume that the vertical swimming height (dotted line) of larvae is linear with time (or age) at the population level. The larvae reach the middle water layer (relative depth $y/H = 0.5$) at 0 dph and the water surface (relative depth $y/H = 0$) at 2 dph. Afterward, the vertical position of the larvae decreases linearly with time (or age), and the larvae reach the bottom of the river at 8 dph, and then enter the cover stage.

(C) During the drift stage, the early larvae migrate laterally from the thalweg to the shores and vertically from the bottom to the surface and then down to the bottom. Their longitudinal migration speed at the population level is the same as the current speed calculated by Equation 4, and their lateral and vertical speeds are age dependent for reaching different locations near the shores (red triangle).

(D) Migration stage division corresponding to ontogenetic development of the Chinese sturgeon after hatching (top) (Zhuang, 1999; Zhuang et al., 2002) and linear length growth of juveniles with age (bottom).

See also Figures S2 and S3, Tables 1 and S1, Video S1.

Daily Age (dph)	Migration Stage/Young Fish	Swimming Traits	Relative Water Depth (y/H)	Migration Speed of Fish U (km/day)		Diffusion Coefficient of Fish D (km²/day)
				Pre-GD	Post-GD	
0	Hatchling	Drift with current, accompanied by vertical swimming and transverse swimming up to the water surface and toward the shores due to weak phototaxis	0.5	–	–	–
1	Drift stage/Free-living embryo or early larva		0.25	102.14	73.48	36.3
2			0	78.19	56.25	42.4
3		Drift with current, accompanied by vertical swimming down from the upper water layer to the bottom water layer followed by swimming to the shores due to phototaxis	0.17	52.9	38.06	50.9
4			0.33	32.8	23.59	63.6
5			0.5	17.7	12.74	84.8
6			0.67	7.43	5.34	127.2
7			0.83	1.68	1.21	254.4
8		Enter the bottom water layer in the shores	1	0	0	254.4
–		Sum of drifting distance (km)	–	292.24	210.67	–
9–11	Cover stage/Early larva	Hide in the cracks of riverbed gravel-cobble substrate	1	0	0	254.4
12	Cover stage/Early larva start feeding					
13–18	Cover stage/Late larva					
19–39	Self-migration stage/Late larva	Restart downriver migration along the inshore waters and bottom water layer relying on the swimming ability, although affected by current	Bottom of riverbed	Equation 12 in Transparent Methods		Equation 20 in Transparent Methods
40–150	Self-migration stage/Juvenile					
150–270	Self-migration stage/Juvenile	Enter tidal-affected region				

Table 1. Division of Migration Stages and Model's Parameters of Juvenile Chinese Sturgeon

Figures 2B and 2C show the larvae's locations in cross-sections of the water layer after hatching. According to the water depth preference of early larvae, we assumed that the vertical swimming distance of the larvae is linear with time (or age) at the population level. The larvae reach the middle water layer (relative depth $y/H = 0.5$) at 0 dph and water surface (relative depth $y/H = 0$) at 2 dph. Afterward, the vertical position of the larvae decreases linearly with time (or age), and the larvae reach the bottom of the river at 8 dph and then enter the cover stage. Table 1 shows the migration speed (U_1) and the diffusion coefficient (D_1) of larvae at different ages. We have applied the perched water layer of relative depth value y/H obtained in the laboratory (Zhuang, 1999; Zhuang et al., 2002) to the Yangtze River. This method has been supported by Kynard et al. (2007) and Braaten et al. (2008), whereby the vertical distribution of larval pallid sturgeons in laboratory and field experiments show similar characters. The diffusion coefficient increases rapidly in the drift stage, indicating that the larvae disperse quickly to avert the threat of predators.

(2) Cover stage (9–18 dph): Zhuang (1999) and Zhuang et al. (2002) reported that the early larvae begin to hide in the cracks of gravel-cobbles at 7 dph and reach peak individual numbers at 8–10 dph. The probability of hiding at 11 dph starts to decrease until 18 dph, when most of the larvae leave the cracks. In this stage, the larvae initiate feeding when the yolk sac is exhausted at 11–12 dph. An increase in the duration of the capability to resist the current is observed at the onset of exogenous feeding by the larvae. We considered that the larvae hide in cracks at the riverbed from 9 to 18 dph in the lower reaches of the spawning ground but show diffusion behavior owing to the local eddies. Therefore, the time-averaged velocity of the current (U_2) = 0. We took the diffusion coefficient at 7 dph when larvae are near the bottom of the river bed as $D_2 = 254.4$ km²/day (Table 1, also see Transparent Methods), indicating that the larvae

are scattered as far as possible in the cover stage, especially after the start of feeding, to reduce the risk of predation.

(3) Self-migration stage (after 18 dph): Based on studies in the laboratory by Zhuang (1999) and Zhuang et al. (2002), we inferred that, after 18 dph, the late larvae begin their inshore migration downstream while searching for rich food in rearing areas on their way. In the self-migration stage, the juveniles' path can be divided into the river region, where the current is mainly determined by the upstream inflow, and the tidal-affected region, where the current is affected by both upstream inflow and the tidal current. Because of the spatiotemporal variability of runoff and the tidal current, the lengths and the origin-destination of the two regions vary with the complicated interaction of river runoff and tidal current. The stronger the runoff is, the more powerfully the freshwater suppresses the tidal current. Then the upper boundary of the tidal-affected region moves downward, or vice versa. Xu et al. (2012) found that the upper boundary of the tidal-affected region should be between Wuhu and Zhenjiang. According to calculations considering the combination of flood season and high tide, the average cross-section velocity below Nanjing is reduced by the tidal current. The time for juveniles to reach the estuary is between May and August. Therefore, the tidal effect on the migration speed of juvenile should occur below Nanjing (347 km). Wang et al. (2014) showed that the downriver speed of juvenile Chinese sturgeon decreased when they entered the tidal-affected region. Therefore, to simplify the calculations, we regarded Nanjing as the fixed demarcation point between the river region and the tidal-affected region, where the latter can be further divided into freshwater and brackish subregions (Figures 1C and S1).

Classification methods of the fish swimming speed correspond to different definitions and indices of swimming speed, such as critical swimming speed, maximum sustained swimming speed, and optimum cruising swimming speed (Wang et al., 2010). The migration speed (U) in the MDM refers to the swimming speed of the juveniles over the ground at the population level, which is distinguished from the critical swimming speed that is widely used. Based on the growth data of juvenile Chinese sturgeon (Zhuang et al., 2002; He et al., 2013), the relationship between full length and age of a juvenile is expressed as $L = 0.1256 t + 1.4338$. Other species of sturgeon show a similar linear relationship (Braaten and Fuller, 2007). When the juveniles are less than 12.5 months old, the critical swimming speed and the age can be approximately expressed as a linear relationship, despite the difference in test conditions leading to different formulae (Figure S2C). Therefore, we assumed that the migration speed of juveniles is a linear function of age (Figure S2D).

Owing to the limitations of observation techniques, it is difficult to obtain from the field environment the spatiotemporal distribution of migration speed (U_3) of juveniles after 18 dph. Theoretically, the swimming ability of the fish is related to their body condition, including health, body length, tail length, and swing frequency, as well as environmental conditions such as water temperature, velocity, and velocity gradient of the current. We used the fishing and mark-recapture data to obtain similar expressions for the speed function and took the average value as the migration speed of juveniles. Meanwhile, we assumed that the migration speed of juveniles from Nanjing to the estuary is reduced by 30%, and we introduced a tidal influence coefficient (γ) in the tidal-affected region. In the self-migration stage, the diffusion coefficient (D_3) is synthetically determined by the swimming ability and the current speed; the current effect on the juvenile migration speed decreases with age. Therefore, we divided D_3 into two parts: the fish-related diffusivity, denoted by D_f, is determined by the juvenile swimming ability and increases with age, and the current-related diffusivity (D_w) is determined by the current speed and is attenuated with an increase in age. We have estimated D_3 in the self-migration stage ($t > 18$ dph) (see Transparent Methods).

Vital Functions of Weak Swing or Swimming of Larval Fish

The spawners of Chinese sturgeon usually lay adhesive eggs in the rapids. The eggs are deposited while being fertilized and then adhere to the rocks at the bottom of spawning ground, normally attracting large numbers of predators. Five days later, the fertilized eggs hatch, and the early larvae start to drift downriver with the current. The early larvae, due to their phototaxis, skillfully utilize the bend flow and the mechanical interaction between their weak swing and the current, amplifying the weak swing by dint of the water current, to reach the littoral zone at the end of the drift stage (Figure 2). The larvae have evolved a unique swimming pattern as a survival tactic. Conversely, if the larvae had drifted with the maximum water velocity of the thalweg without approaching the shore by weak swing, they would have reached the brackish subregion at the estuary within about half a month and then would have certainly died, as they would be unable to feed
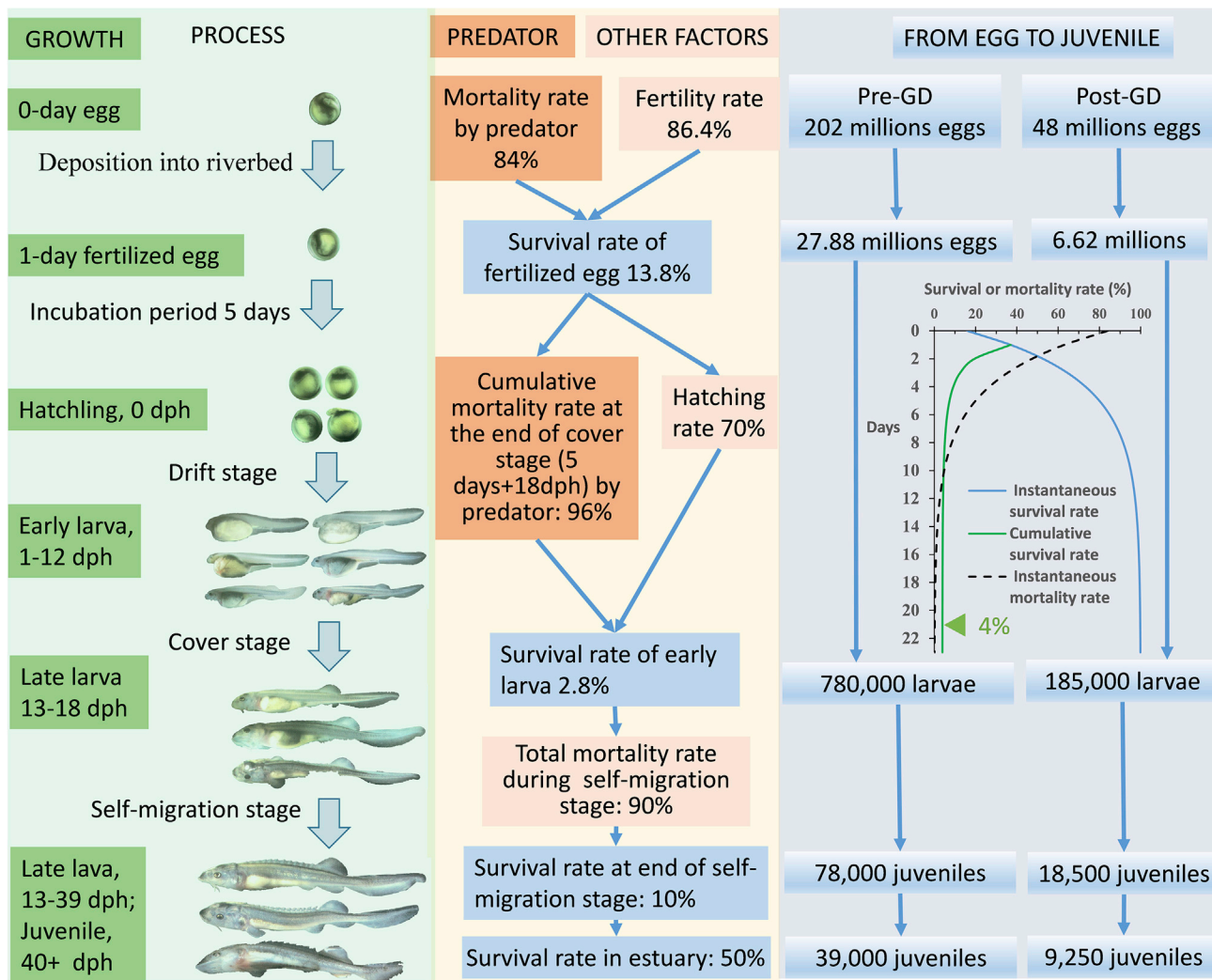
Figure 3. The Mortality Rate of Wild Young Chinese Sturgeon After Spawning in the Yangtze River

To study the migration process of young Chinese sturgeon in the Yangtze River, we need to assume the initial number of sturgeon eggs and then estimate the number of young fishes through the age-specific mortality rate as the initial conditions for the calculations. The egg production of the fish is usually estimated by sampling predators and dissection statistics of the eggs devoured, but this results in a broad range of annual variation (Wei, 2003; Chang, 1999; Yu et al., 2002), even when the pre-GD had a stable adult population size. According to our estimation of the population size of adult Chinese sturgeon (Huang et al., 2017; Huang and Wang, 2018), the GD construction had resulted in a reduction of the yearly effective breeding population from 1,009 individuals of pre-GD to 244 post-GD, corresponding to 24.2% of the original. Considering the sex ratio (1:1) of the fish and the average fecundity (400,000 eggs per female), the total egg production for pre-GD and post-GD are 202 million eggs and 48.8 million eggs, respectively. See also Transparent Methods and Video S1.

or would be too small to adapt to the saltwater environment. Here, we highlight that the weak swing of early larvae or swimming ability of larvae, ignored in the past, plays a crucial role in leaving the rapids and in anti-predator behavior. The larvae prefer shallow waters with rich food for survival and feeding.

Figure 3 shows that the total mortality rate of Chinese sturgeon from egg to 9 months of age is about 99.98% before they enter the sea, which is consistent with the egg-to-1-year mortality rate range of 99.96%–100% for the Gulf sturgeon (*A. oxyrinchus desotoi*) (Pine et al., 2001). The mortality of young Chinese sturgeon in the Yangtze River plays a crucial role in population recovery. Their mortality risk sources change from mostly predators in the drift and cover stages to complex factors such as starvation (Caroffino et al., 2008), water pollution (Hu et al., 2009), bycatch (Chang, 1999), and a variety of hydrological conditions, including the effects of saltwater in the estuary (He et al., 2009; Zhao et al., 2011, 2015) in the self-migration stage. Before the self-migration stage, the survival rate of larvae is the lowest at 0.39%, mainly

owing to predators devouring eggs and larvae. Therefore, for the wild larvae of Chinese sturgeon, their anti-predator behavior in the drift and cover stages is the most important factor affecting the population recovery; this also underlines the ecological significance of weak swing or free swimming of the wild larvae.

Parametric Traits of Migration Stages

Figures 4A and 4B show the migration speed and diffusion coefficient of juveniles over time in the down-river migration process. First, after hatching the early larvae leave the bottom and rapidly depart the spawning ground with the water current. The larvae's drift speed mainly depends on the velocity distribution of water flow and the spatial position of the larvae accompanying their weak vertical and horizontal swimming ability. The diffusion coefficient increases rapidly in the drift stage, indicating that the larvae disperse quickly to avoid predators. Second, during the cover stage, the larvae are mainly distributed in the inshore riverbed, hiding in cracks of gravel-cobbles and starting to feed at 11–12 dph. At this stage, the larvae stay in the bottom substrate without time-averaged migration velocity. However, the diffusion coefficient reaches the maximum owing to the inhomogeneity of the boundary layer with turbulent eddies, indicating that the larvae are scattered as far as possible, especially after the start of feeding, to reduce the risks of predation and food competition. Third, during the self-migration stage, the larvae start the course of migration along the inshore waters and search for food in the rearing area on the way. They move randomly in the Yangtze River at the individual level but always move downstream at the population level. With the increase of age, the larvae's swimming ability grows and the effect of current on their migration speed gradually weakens. The fish-related diffusivity is proportional to age squared, and the constant Peclet number of the fish migration shows that the convective term is about nine times the fish-related diffusivity term in the self-migration stage of juveniles. Overall, the migration speed and diffusion coefficient of juveniles gradually increase. After entering the tidal-affected region (below Nanjing), the juveniles slow down. However, the diffusion coefficient increases with the age of the fish.

The downriver migration reflects some characteristics successively as drifting with the current → hiding → self-migrating (acceleration-deceleration) along the inshore waters and indicates certain gradually transforming manners, from passive movement (drifting with the flow) to active swimming (self-migrating), and from the rapids of the thalweg to the quiet flow area of the littoral zone. Furthermore, we revealed that the spatiotemporal density of the juveniles evolved along the migration path into a normal distribution.

Panoramas of Migration Processes

Regardless of the impact of the GD on juvenile mortality, we can estimate the number of surviving larvae or juveniles at all stages (Figure 3). At the end of the cover stage, the number of early larvae used as the initial conditions of MDM calculation was 780,000 individuals pre-GD and 185,000 post-GD. Figure 3 shows that pre-GD there were 39,000 individuals entering the sea and post-GD the number was 9,250. Pine et al. (2001) reported that the annual mortality rates of Gulf sturgeon (*A. oxyrinchus desotoi*) were 25% for those 1–3 years old and 16% for those 4–25 years old. Assuming that the annual mortality rates of Chinese sturgeon in the sea are the same as those of Gulf sturgeon, we can estimate the maximum number of the potential recruit population in 18 years (average age of female and male adults, corresponding total survival rate of 3%) to be 1,170 individuals pre-GD and 278 post-GD, equivalent to the numbers of annual recruitment. These numbers are consistent with the theoretical estimates (Huang and Wang, 2018) and the estimated results from the field tests in the early years of post-GD (Chang, 1999; Wei, 2003). In a word, the total natural survival rate from eggs to mature adults that can live to return to the Yangtze River averaged about 6×10^{-6} for the wild Chinese sturgeon, implying that each female spawner with a fecundity of 1 million eggs can contribute only six surviving recruits.

Figure 4C shows that in pre-GD, the peak density of juveniles at Nanjing occurred in July, meaning that they were entering the tidal-affected region at 8 months old when their pioneers arrived at the estuary. The peak time of the fish reaching the estuary (Shanghai) was in August when they were 9 months old. The final time for the juveniles to leave the estuary was in early August. Figure 4D shows that post-GD there was a peak density at Nanjing at the beginning of May, when the fish were 5 months old, with pioneers reaching the estuary. However, the peak time at the estuary was mid-June, when fish were at the age of 6.5 months, and the time to enter the sea was in late August. Figures 4C and 4D show that the density distribution curve of juveniles gradually flattens along the path and bulges in the estuarine area, showing an aggregation effect of the fish; the GD has shortened the migration distance of Chinese sturgeon by 1,175 km, causing the
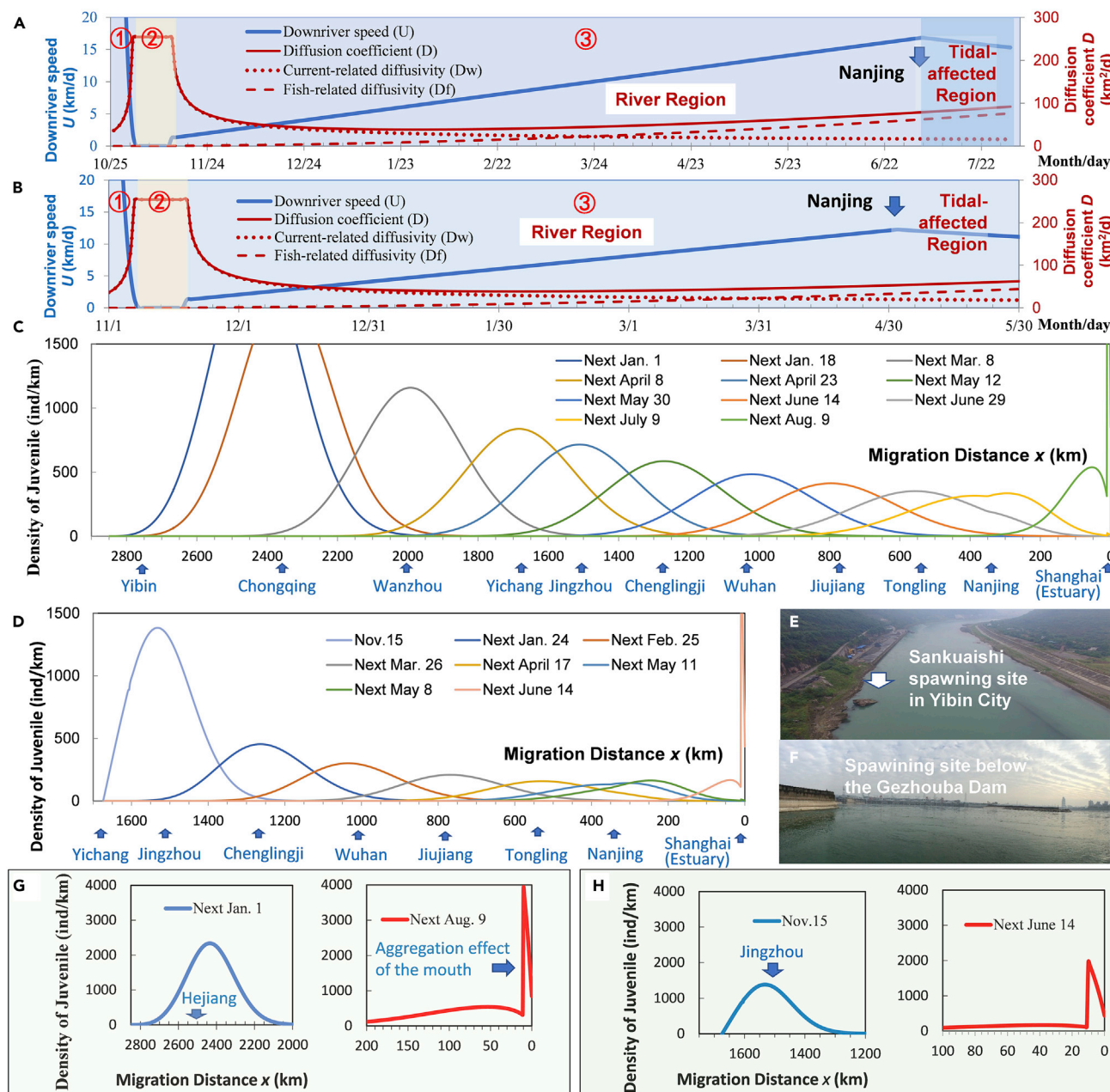
Figure 4. Model Parameters and Calculated Results of Downriver Migration Processes of Young Chinese Sturgeon in the Yangtze River

(A and B) Migration velocity U and diffusion coefficient D of young Chinese sturgeon varied with time in the ① drift stage; ② cover stage; and ③ self-migration stage. Pre-GD (A) was similar to post-GD (B), but with the difference in spawning ground, the flow velocity was higher in the upper Yangtze River than that below the GD in the middle reach of the Yangtze River.

(C and D) Normal migration processes of juvenile Chinese sturgeon for pre-GD (C) and post-GD (D), indicating that the peak density of juveniles passed through the main cities.

(E) Sankuanshi, one of the three famous spawning sites pre-GD, is located about 45 km upstream of Yibin City.

(F) The standing spawning site of post-GD below the GD.

(G and H) Comparison of juvenile densities at the starting site of the self-migration stage and in the river mouth for pre-GD (G) and post-GD (H), showing that the aggregation effect of the juveniles in the 10-km-long East Beach of Chongming Island occurred and that the GD has caused a considerable drop in the population size of juveniles.

See also Figures S1–S4, Tables 1 and S1–S3, Video S1.

juveniles to reach the estuary 1.5 months earlier while posing an extra mortality risk related to the saltwater adaption.

We can estimate that pre-GD had the migration distance of the drift stage for 292 km, from the spawning site at Sankuaishi (Figure 4E) to the hiding site between Hejiang in Sichuan Province and Lanjiatuo in Chongqing Municipality. However, post-GD had the fish drifting for 211 km, from the standing spawning site below the GD (Figure 4F) to a hiding site between Jinzhou and Shishou in Hubei Province (Figure 1A), which was verified empirically by frequent bycatch of local fishermen. The number of larvae hatched post-GD was only a quarter of that pre-GD, because the GD reduced the size of the spawning ground. Therefore, the peak density of juveniles post-GD (Figure 4G) was only one-half of that pre-GD (Figure 4H) in the estuary.

Finally, we describe the overall life cycle of Chinese sturgeon in the Yangtze River pre- and post-GD, involving the migration of wild adult and young fish upriver or downriver (Figure 5A). Meanwhile, we demonstrate that the gonadal development stage of Chinese sturgeon is a vital sign of the fish entering and departing the estuary (Figure 5B) as a result of evolutionary adaption.

DISCUSSION

Vertical Distribution of Juveniles

Data concerning the vertical distribution of juvenile Chinese sturgeon is lacking for inshore waters. Caroffino et al. (2009) studied the vertical distribution of the larval lake sturgeon (*A. fulvescens*) at a total length of 16–22 mm and found an uneven vertical distribution; the density of the upper layer was higher than that of the lower layer. In a 150-cm deep artificial stream tube, shortnose sturgeon (*A. brevirostrum*) larvae moved downstream, but the majority swam above the bottom at an average height of 100 cm (Kynard and Horgan, 2002). In a similar stream tube experiment, pallid sturgeon (*Scaphirhynchus albus*) and shovelnose sturgeon (*S. platorhynchus*) larvae drifted mostly downstream at the surface (Kynard et al., 2002), whereas white sturgeon (*A. transmontanus*) larvae moved downstream at an average depth of 4–58 cm above the bottom (Kynard and Parker, 2005). Therefore, we inferred that the perched waters of juveniles are within 2–5 m in depth during the self-migration stage, and that the early juveniles mainly migrate along with the bottom layer (Zhuang et al., 2002). With the age-dependent increase of swimming ability, the juveniles switch to an even distribution vertically in the inshore waters. Here we reflect the average swimming behavior of the young fish at a large timescale, without considering the details of diel rhythm.

Backcasting Estimation of the New Spawning Place

The Yangtze cascade dams have had a significant impact on the Chinese sturgeon, which has had its spawning activities decrease from continuous to occasional since the operation of the Three Gorges Dam in 2008 and have disappeared since the Xiluodu Dam in 2013 (Wu et al., 2017b). Despite spawners being mainly distributed within the 30 km below the GD during the spawning season, a small number of the fish may also be scattered in the Wuhan-Jiujiang section (Huang and Wang, 2018). Therefore, a large amount of spawning activity in the traditional spawning ground may cover up the fragmentary, small numbers of spawning fish in other sites. We can infer that other spawning sites may exist if there are appropriate water temperatures, substrates, and hydrological factors. Only four wild juveniles were caught in the estuary on April 16–25, 2015, earlier than normal and far less in number than in previous years. This demonstrated that a small amount of spawning activity in 2014 occurred in an unknown place downstream far from the GD, instead of at the traditional site (Zhuang et al., 2016). Here we estimate that the spawning area in 2014 was probably located between Wuhan and Jiujiang, most likely in the Huangshi section. If we have more collected data in the estuary, such as the peak time of juvenile density, we can calculate backward the spawning time and site more accurately.

Improvements of Artificial Restocking

On 4 January, 1981, the GD dammed the Yangtze River, causing a hot dispute over if—and by how much—the GD may have influenced the river's aquatic life. From then on, China listed the Chinese sturgeon as the sole target of GD's fish rescue and started an artificial restocking program as a remedial measure. From the mid-1980s to the present, more than 6 million individuals of different sizes have been continually released into the Yangtze River, but this has so far achieved little in the recruitment of the population due to an inappropriate strategy—''emphasis on reproduction technique and neglect of post-release
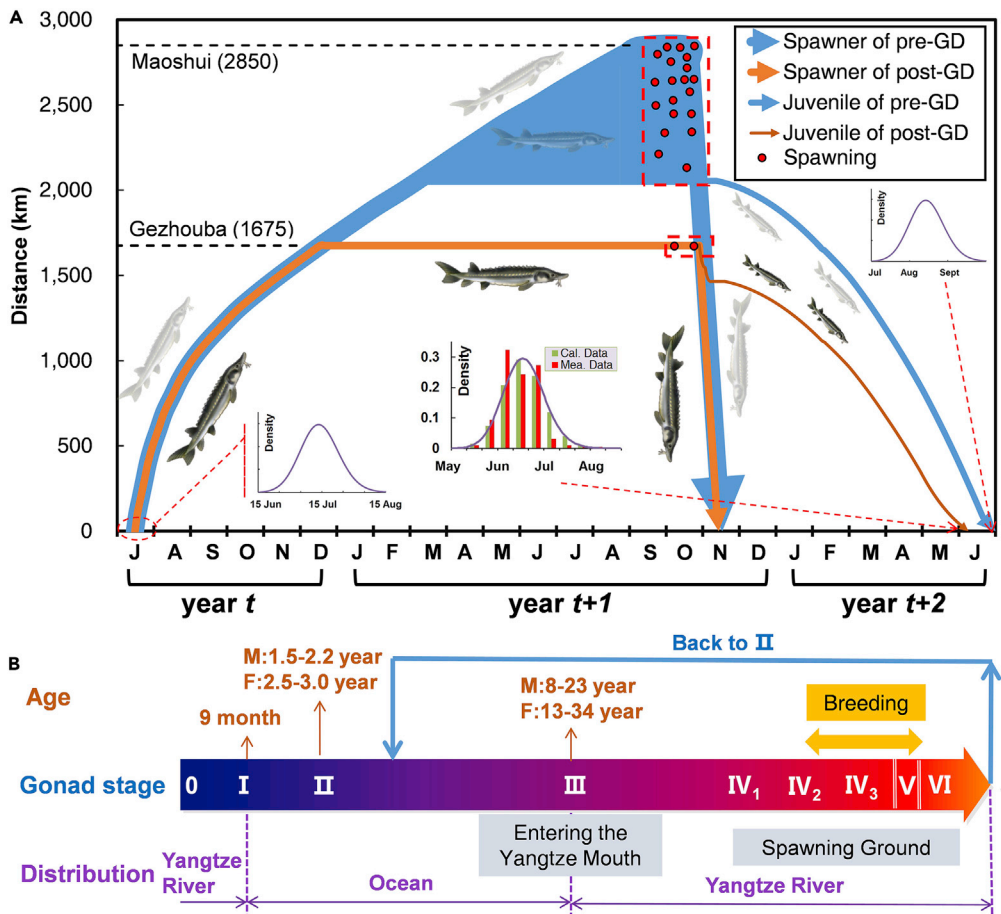
Figure 5. Chinese Sturgeon Life Cycle and Gonadal Development

(A) Overall life cycles of the migration processes for the adult and the young Chinese sturgeon pre- and post-GD. The red dotted rectangle indicates the location and size of the spawning ground. The adult Chinese sturgeon entered the Yangtze estuary from June to August (normally distributed with July 15 as the median) each year. In the following autumn, reproduction was completed under suitable hydrological conditions. After spawning, the adults quickly migrated to the ocean. The GD shortened the downriver migration distance by 1,175 km; thus, the adults reached the estuary 10 days earlier than normal (Huang and Wang, 2018). The downriver migration of juveniles takes about 9 months, and the occurrence time of juveniles in the estuary shows a normal distribution. The GD shortened the migration time of juveniles to reach the estuary by 1.5 months. On the abscissa (in order): J, July; A, August; S, September; O, October; N, November; D, December; J, January; F, February; M, March; A, April; M, May; J, June.

(B) Gonadal development in the Yangtze and the sea. After birth in October-November, the larvae move downriver stepwise along the path at gonadal stage 0. Gonads reach stage I at 9 months old when the larvae leave the river mouth in August-September. In the ocean, at 1.5–2.2 years (males) or 2.5–3.0 years (females) old, gonads develop into stage II, and at least at age 8 years for males or 13 years old for females into stage III, at which the fishes become spawners and start to enter the Yangtze River in June-August. They go upstream to reach the spawning ground while there is complete gonadal development from stage III to IV. Spawners remain in the spawning ground for 3 months until the gonads grow from stage IV to IV2 and become mature. Gonads develop fast from stages IV2 to VI with suitable hydrological stimuli, and then mating occurs. After breeding, gonads drop from stages VI to II (YARSG, 1988; Chen et al., 2004; Huang and Wang, 2018).

behavior," resulting in a lack of effective evaluation of the artificial restocking program (Brown and Day, 2002). For example, the traditional view states that the larger or older the individual released is, the higher the survival rate; is this true? How can one balance the economics of hatchery-reared fish number or size and their post-release survival rate for a cost-effective outcome? Wu et al., (2017a) reported that 61 cultured juvenile Chinese sturgeon 3 years of age were tagged and released below the GD on April 12, 2015. The fish migrated downriver 1,500 km, and finally only 21 individuals (34%) reached the Yangtze estuary half a month later. As a result of exceeding expectations, they were unable to explain why 66% of the

tagged fish were "lost" during their seaward migration. Similar situations occurred in the subsequent years.

Based on the laboratory results of juvenile hybrid sturgeon (*Huso duricus* ♂ × *A. schrencki* ♀) (Li et al., 2011) and Chinese sturgeon (Zhuang et al., 2017), there are four main movement patterns in the flowing environment of juvenile fish: upstream, still, countercurrent backward, and drift-downward movements. The upstream movement indicates that juvenile fish swim against the current and move forward owing to their rheotaxis; the still movement means that the fish remains in a motionless state over the ground, and the countercurrent backward movement pattern indicates receding relative to the ground. The only pattern of downstream swimming is the drift-downward movement, indicating that the juvenile fish move downstream with the current without adverse-current behavior. We can assume that the individual juvenile Chinese sturgeon in the wild will display the four movement patterns at different velocities of water flow during the self-migration stage, namely, upstream, still, countercurrent backward, and drift-downward movements (Figures S3A–S3E). Among the four-movement patterns, the predominance of the counter-current backward in a running water environment implies that a juvenile must consume a great deal of energy compared with a drift-downward movement that would save energy. Experiments in the labora-tory reported that an individual juvenile usually shows complex diurnal swimming behavior (Kynard et al., 2002; Zhuang et al., 2002). However, the juveniles generally move downstream at an average daily swimming speed at the population level (Figure S3F). We can infer that the released fish migration down-river is characterized by the four movement patterns mentioned earlier and that the juveniles must consume a great deal of energy. If the Yangtze River cannot provide suitable food along the way for the released fish, this will lead to high mortality. Therefore, improving post-release behavioral perfor-mance requires understanding the migration process. The findings of this paper can contribute to the improvement of artificial restocking for the endangered Chinese sturgeon and other anadromous fish species in the world.

Limitations of the Study

Here, we reflect on the migration characteristics of juvenile fish at a daily scale and the population level. The swimming behavior at the individual level, or hourly scale or segment scale, remains unclear. For the self-migration stage, if we can characterize the distribution of juvenile-specific bait-organisms along the Yangtze River, we can combine the MDM with the habitat model to obtain a more detailed spatiotemporal distribution of juvenile fish. In any event, the findings of this paper can provide useful information to deter-mine the key areas of protection for the management of juvenile fish along the Yangtze River, and the model can be used to assess the influence of dams on the migration of juvenile fish.

Additionally, we do not consider the influence of changing river hydrological conditions on the migration process or the navigational mechanism of the long-distance migration. Studies have shown that long-dis-tance migrants can use geomagnetic information to navigate. Species studied include Pacific salmon (*Oncorhynchus* spp) (Putman et al., 2014b), Chinook salmon (*Oncorhynchus tshawytscha*) (Putman et al., 2018), steelhead trout (*Oncorhynchus mykiss*) (Putman et al., 2014a), loggerhead sea turtles (*Caretta care-tta*) (Putman and Mansfield, 2015), and European eels (*Anguilla anguilla*) (Naisbett-Jones et al., 2017). An inherited magnetic map (i.e., an ability to extract positional information from Earth's magnetic field) exists in these organisms to guide their migration processes. These above-mentioned two components merit further study to improve our model for the Chinese sturgeon and other migratory species.

METHODS

All methods can be found in the accompanying Transparent Methods supplemental file.

DATA AND CODE AVAILABILITY

Raw data for the model parameters and calculated results (Figure 4) and their Matlab software code are available online via a Mendeley Data repository with DOI links at https://doi.org/10.17632/gyg6gg4mtk.1.

SUPPLEMENTAL INFORMATION

Supplemental Information can be found online at https://doi.org/10.1016/j.isci.2019.08.029.

REFERENCES

Auer, N.A., and Baker, E.A. (2002). Duration and drift of larval lake sturgeon in the Sturgeon River, Michigan. J Appl. Ichthyol. *18*, 557–564.

Bao, D.Y., and Zhu, J.R. (2017). The effect of river regime changes in the Changjiang Estuary on hydrodynamics and salinity intrusion in the past 60 years (III. Saltwater intrusion). Haiyang Xuebao *39*, 1–15.

Braaten, P.J., and Fuller, D.B. (2007). Growth rates of young-of-year shovelnose sturgeon in the Upper Missouri River. J. Appl. Ichthyol. *23*, 506–515.

Braaten, P.J., Fuller, D.B., Holte, L.D., Lott, R.D., Viste, W., Brandt, T.F., and Legare, R.G. (2008). Drift dynamics of larval pallid sturgeon and shovelnose sturgeon in a natural side channel of the upper Missouri River, Montana. N. Am. J. Fish Manag. *28*, 808–826.

Braaten, P.J., Fuller, D.B., Lott, R.D., Ruggles, M.P., Brandt, T.F., Legare, R.G., and Holm, R.J. (2012). An experimental test and models of drift and dispersal processes of pallid sturgeon (*Scaphirhynchus albus*) free embryos in the Missouri River. Environ. Biol. Fish *93*, 377–392.

Brown, C., and Day, R.L. (2002). The future of stock enhancements: lessons for hatchery practice from conservation biology. Fish Fish. *3*, 79–94.

Caroffino, D.C., Sutton, T.M., and Daugherty, D.J. (2009). Assessment of the vertical distribution of larval lake sturgeon drift in the Peshtigo River, Wisconsin, USA. J. Appl. Ichthyol. *25* (s2), 14–17.

Caroffino, D.C., Sutton, T.M., and Lindberg, M.S. (2008). Abundance and movement patterns of age-0 juvenile lake sturgeon in the Peshtigo River, Wisconsin. Environ. Biol. Fish. *86*, 411–422.

Chang, J.B. (1999). Structure and Dynamics of the Spawning Stock of Chinese Sturgeon, Acipenser Sinensis, in the Yangtze River, Ph.D. thesis (Institute of Hydrobiology, Chinese Academy of Sciences). http://ir.ihb.ac.cn/handle/342005/12532.

Chen, X.H., Wei, Q.W., Yang, D.G., Zhu, Y.J., and Liu, Y. (2004). Histological studies on gonadal origin and differentiation of cultured *Acipenser sinensis*. J. Fish. Sci. China *28*, 633–639.

Erwin, S.O., and Jacobson, R.B. (2015). Influence of channel morphology and flow regime on larval drift of Pallid sturgeon in the lower Missouri River. River Res. Appl. *31*, 538–551.

Fossette, S., Gleiss, A.C., Chalumeau, J., Bastian, T., Armstrong, C.D., Vandenabeele, S., Karpytchev, M., and Hays, G.C. (2015). Current-oriented swimming by jellyfish and its role in bloom maintenance. Curr. Biol. *25*, 342–347.

He, X., Lu, S., Liao, M., Zhu, X., Zhang, M., Li, S., You, X., and Chen, J. (2013). Effects of age and size on critical swimming speed of juvenile Chinese *Acipenser sinensis* at seasonal temperatures. J. Fish Biol. *82*, 1047–1056.

He, X., Zhuang, P., Zhang, L., and Xie, C. (2009). Osmoregulation in juvenile Chinese sturgeon (*Acipenser sinensis* Gray) during brackish water adaptation. Fish Physiol. Biochem. *35*, 223–230.

Hu, J.Y., Zhang, Z.B., Wei, Q.W., Zhen, H.J., Zhao, Y.B., Peng, H., Wan, Y., Giesy, J.P., Li, L.X., and Zhang, B. (2009). Malformations of the endangered Chinese sturgeon, *Acipenser sinensis*, and its causal agent. Proc. Natl. Acad. Sci. U S A *106*, 9339–9344.

Huang, Z.L., and Wang, L.H. (2018). Yangtze dams increasingly threaten the survival of the Chinese sturgeon. Curr. Biol. *28*, 3640–3647.

Huang, Z.L., Wang, L.H., and Ren, J.Y. (2017). Study on the spawning population fluctuation of Chinese sturgeons around the closure of Gezhouba Dam. Sci. Sin. Tech. *47*, 871–881.

Kynard, B., and Horgan, M. (2002). Ontogenetic behavior and migration of Atlantic sturgeon, *Acipenser oxyrinchus oxyrinchus*, and shortnose sturgeon, *A. brevirostrum*, with notes on social behavior. Environ. Biol. Fish *63*, 137–150.

Kynard, B., and Parker, E. (2005). Ontogenetic behavior and dispersal of Sacramento River white sturgeon, *Acipenser transmontanus*, with a note on body color. Environ. Biol. Fish *74*, 19–30.

Kynard, B., Henyey, E., and Horgan, M. (2002). Ontogenetic behavior, migration, and social behavior of pallid sturgeon, *Scaphirhynchus albus*, and shovelnose sturgeon, *S. platorynchus*, with notes on the adaptive significance of body color. Environ. Biol. Fish *63*, 389–403.

Kynard, B., Parker, E., Pugh, D., and Parker, T. (2007). Use of laboratory studies to develop a dispersal model for Missouri River pallid sturgeon early life intervals. J. Appl. Ichthyol. *23*, 365–374.

Kynard, B., Wei, Q.W., and Ke, F.E. (1995). Use of ultrasonic telemetry to locate the spawning area of Chinese sturgeon. Chin. Sci. Bull. *40*, 668–671.

Li, D., Lin, X.T., Zhu, Z.M., and Yi, M.M. (2011). Effects of flow rate on swimming states and activity metabolism in juvenile hybrid sturgeon. Acta Hydrobiologica Sinica *35*, 578–585.

Lin, Y.B. (2008). A Preliminary Study on the Distribution and Downstream Migration of the Reproductive Stock of Chinese Sturgeon in the Yangtze River in Nonbreeding Season, Master thesis (Huazhong Agricultural University). https://doi.org/10.6084/m9.figshare.6798401.

Naisbett-Jones, L.C., Putman, N.F., Stephenson, J.F., Ladak, S., and Young, K.A. (2017). A magnetic map leads juvenile European eels to the Gulf Stream. Curr. Biol. *27*, 1236–1240.

Pine, W.E., III, Allen, M.S., and Dreitz, V.J. (2001). Population viability of the Gulf of Mexico sturgeon: inferences from capture-recapture and age-structured models. Trans. Am. Fish. Soc. *130*, 1164–1174.

Putman, N.F., and Mansfield, K.L. (2015). Direct evidence of swimming demonstrates active dispersal in the sea turtle "lost years". Curr. Biol. *25*, 1221–1227.

Putman, N.F., Lumpkin, R., Sacco, A.E., and Mansfield, K.L. (2016). Passive drift or active swimming in marine organisms? Proc. Roy. Soc. B Biolo. Sci. *283*, 20161689.

Putman, N.F., Meinke, A.M., and Noakes, D.L. (2014a). Rearing in a distorted magnetic field disrupts the 'map sense' of juvenile steelhead trout. Biol. Lett. *10*, 20140169.

Putman, N.F., Scanlan, M.M., Billman, E.J., O'Neil, J.P., Couture, R.B., Quinn, T.P., Lohmann, K.J., and Noakes, D.L. (2014b). An inherited magnetic map guides ocean navigation in juvenile Pacific salmon. Curr. Biol. *24*, 446–450.

Putman, N.F., Scanlan, M.M., Pollock, A.M., O'Neil, J.P., Couture, R.B., Stoner, J.S., Quinn, T.P., Lohmann, K.J., and Noakes, D.L. (2018). Geomagnetic field influences upward movement of young Chinook salmon emerging from nests. Biol. Lett. *14*, 20170752.

Stoll, S., and Beeck, P. (2012). Larval fish in troubled waters — is the behavioral response of larval fish to hydrodynamic impacts active or passive? Can. J. Fish Aquat. Sci. *69*, 1576–1584.

The Yangtze Aquatic Resources Survey Group (YARSG) (1988). The Biology of the Sturgeon in the Yangtze and Their Artificial Propagation (Chengdu: Sichuan Scientific and Technical Publishing House). https://doi.org/10.6084/m9.figshare.6794288.

Wang, C.Y., Du, H., Zhang, H., Wu, J.M., Liu, Z.G., and Wei, Q.W. (2014). Migration of juvenile and sub-adult Chinese sturgeon *Acipenser sinensis* Gray, 1835 in the Yangtze River, China below the Gezhouba dam. J. Appl. Ichthyol. *30*, 1–6.

Wang, C.Y., Wei, Q.W., Kynard, B., Du, H., and Zhang, H. (2012). Migrations and movements of adult Chinese sturgeon *Acipenser sinensis* in the Yangtze River. China. J. Fish. Biol. *81*, 696–713.

Wang, P., Gui, F.K., and Wu, C.W. (2010). Classification of fish swimming speed. J. Fish. Sci. China *17*, 1137–1146.

Wei, Q.W. (2003). Reproductive Behavioral Ecology of Chinese Sturgeon (Acipenser Sinensis Gray) with its Stock Assessment, Ph.D. thesis (Institute of Hydrobiology). http://ir.ihb.ac.cn/handle/342005/19195.

Wu, J.M., Wang, C.Y., Zhang, H., Du, H., Liu, Z.G., Shen, L., Wei, Q.W., and Rosenthal, H. (2015). Drastic decline in spawning activity of Chinese sturgeon *Acipenser* sinensis Gray 1835 in the remaining spawning ground of the Yangtze River since the construction of hydro dams. J. Appl. Ichth. *31*, 839–842.

Wu, C., Chen, L., Gao, Y., and Jiang, W. (2017a). Seaward migration behavior of juvenile second filial generation Chinese sturgeon *Acipenser sinensis* in the Yangtze River, China. Fish. Sci. *84*, 71–78.

Wu, J.M., Wang, C.Y., Zhang, S.H., Zhang, H., Du, H., Liu, Z.G., and Wei, Q.W. (2017b). From continuous to occasional: small-scale natural reproduction of Chinese sturgeon occurred in the Gezhouba spawning ground, Yichang, China. J. Fish. Sci. China *24*, 425–431.

Xu, X.H., Fan, L.F., and Gu, M.J. (2012). On tidal mark and tidal current mark in the Yangtze River. Port Waterway Eng. *6*, 15–20.

Yang, D.G., Wei, Q.W., Wang, K., Chen, X.H., and Zhu, Y.J. (2005). Downstream migration of tag-released juvenile Chinese sturgeon (*Acipenser sinensis*) in the Yangtze River. Acta Hydrobiologica Sinica *29*, 26–30.

Yi, J.F. (1994). Investigation on juvenile Chinese sturgeon in the Yangtze River. Gezhouba Hydropower *28*, 53–58.

Yu, G.L., Liu, J., Xu, Y.G., and Chang, J.B. (2002). Estimation on abundance of benthonic fishes preying on eggs of Chinese sturgeon in reach below the Gezhouba Dam in the Yangtze River. Acta Hydrobiologica Sinica *26*, 591–599.

Zhao, F., Qu, L., Zhuang, P., Zhang, L., Liu, J., and Zhang, T. (2011). Salinity tolerance as well as osmotic and ionic regulation in juvenile Chinese sturgeon (*Acipenser sinensis* Gray, 1835) exposed to different salinities. J. Appl. Ichthyol. *27*, 231–234.

Zhao, F., Zhuang, P., Zhang, T., Wang, Y., Hou, J., Liu, J., and Zhang, L. (2015). Isosmotic points and their ecological significance for juvenile Chinese sturgeon *Acipenser sinensis*. J. Fish Biol. *86*, 1416–1420.

Zhuang, P., Li, D.P., Zhang, T., Zhang, L.Z., Zhao, F., Hou, J.L., Duan, M., Feng, G.P., Song, W., Shi, X.T., et al. (2017). Environmental Biology of Sturgeons and Paddlefishes—growth, Development and the Environment (Science Press).

Zhuang, P., Zhao, F., Zhang, T., Chen, Y., Liu, J.Y., Zhang, L.Z., and Kynard, B. (2016). New evidence may support the persistence and adaptability of the near-extinct Chinese sturgeon. Biol. Conserv. *193*, 66–69.

Zhuang, P. (1999). Ontogenetic Behavior of Sturgeons (Acipenseridae) with Comments on Evolutionary and Practical Significance, Doctoral thesis (Institute of Hydrobiology, CAS).

Zhuang, P., Kynard, B., Zhang, L., Zhang, T., and Cao, W.X. (2002). Ontogenetic behavior and migration of Chinese sturgeon *Acipenser sinensis*. Environ. Biol. Fish *65*, 83–97.

Supplemental Information

Drifting with Flow

versus Self-Migrating—How Do Young

Anadromous Fish Move to the Sea?

Zhenli Huang
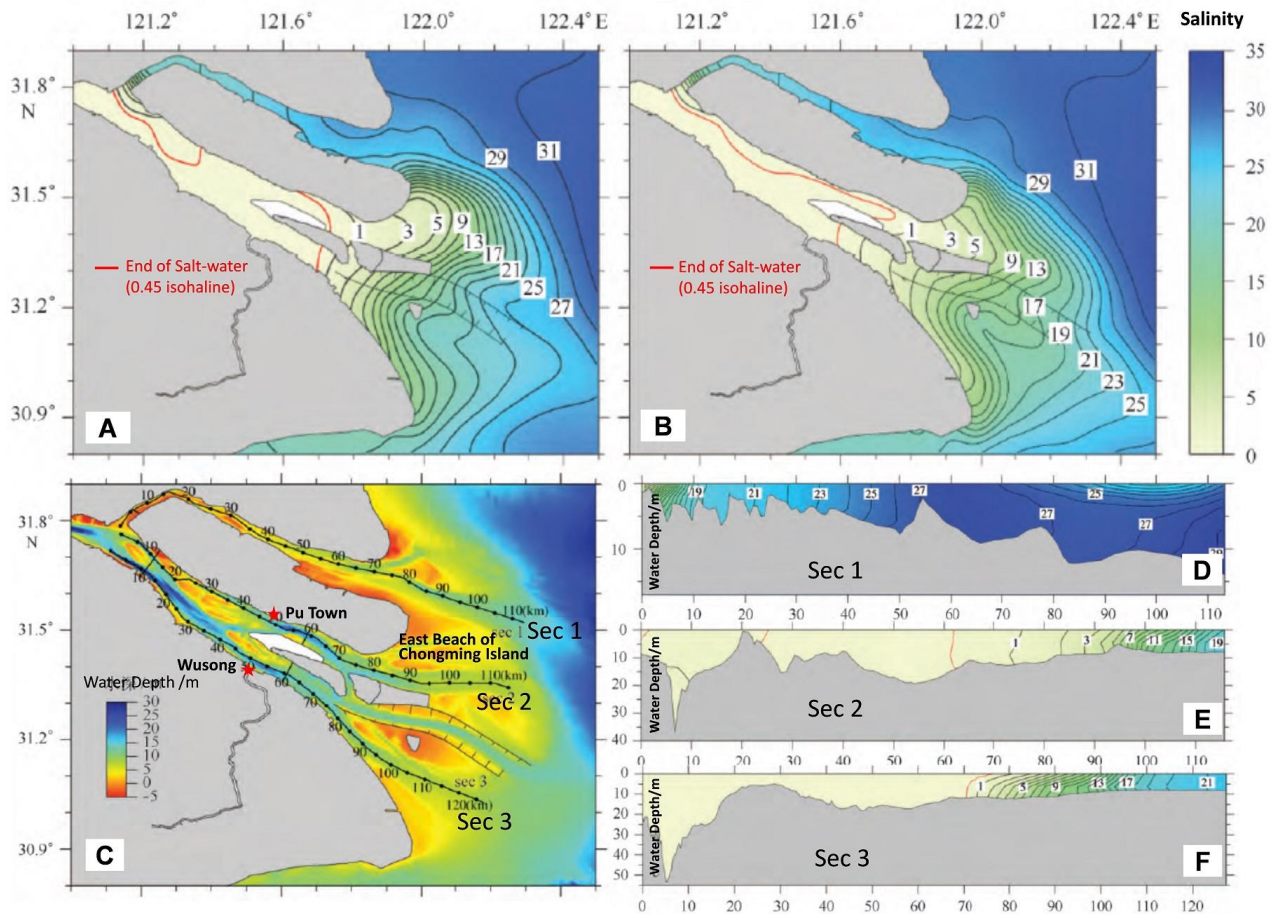
Figure S1. The Saltwater Intrusion of the Yangtze Estuary, Related to Figures 1 and 4. (Bao & Zhu, 2017)

(**A-B**) show the horizontal salinity distributions (psu) of the Yangtze estuary under the spring tide (**A**) and the neap tide (**B**) conditions in January 2012; (**C**) indicates the water depth in the Yangtze estuary and three sections (Sec 1, Sec 2 and Sec 3); (**D-F**) indicate the vertical salinity distribution of the northern branch (Sec 1) and the southern branch (Sec 2 and Sec 3) of the Yangtze estuary, respectively; (**A-F**) show that the saltwater intrusion of the northern branch, all of which are in the saline environment, is more severe than the southern. The upper limit of the salinity effect in the southern branch is at nearby Wusong or Pu Town, about 30 km from Chongming eastern beach.

Figure S2. The Relationship Between Swimming Speed and Age of Juvenile Chinese Sturgeon, Related to Figures 2 and 4.
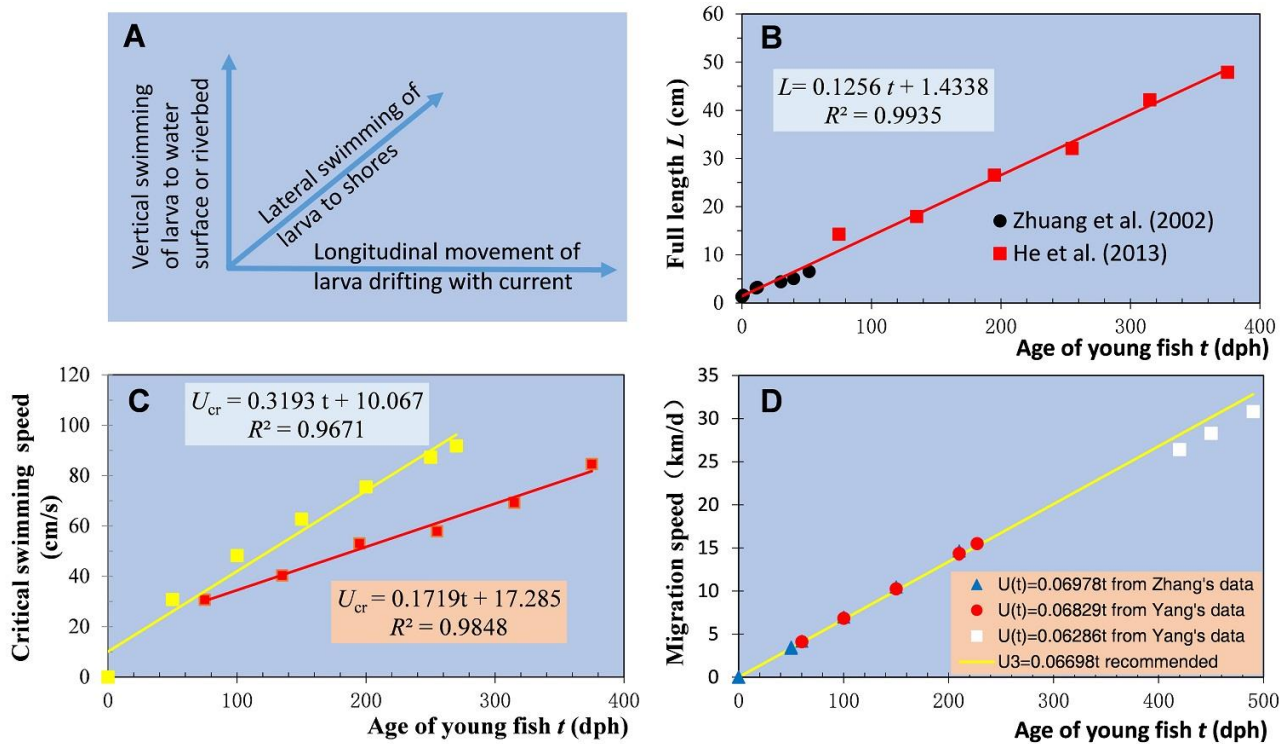
(A) The velocity vector of larvae during the drift stage. Lateral and vertical movements occur in the drift stage due to ontogenetic behavior of early larva and play a crucial role in the antipredator behavior.

(B) The relationship between full length and age of the juveniles shows a linear relationship between critical swimming speed and age, even if different expressions are used. Based on the growth data of juvenile Chinese sturgeon (Zhuang et al., 2002; He et al., 2013), the relationship between full length and age of a juvenile is expressed as L=0.1256 t+1.4338. Other species of sturgeon show a similar linear relationship (Braaten & Fuller, 2007).

(C) The relationship between critical swimming speed and age of the juveniles. Due to differences in time step and velocity increment in the experiment, the critical swimming speed is uncertain. However, it is widely adopted as an index for evaluating the swimming ability of fish due to the small number of test fish and short test time. Duan et al. (2011) measured the relationship between critical swimming speed (U_{cr}) and body length (L) of juvenile Chinese sturgeon as $\log U_{cr} = 0.754 + 0.648 \log L$. According to the relationship between age and body length (**B**), we have obtained $U_{cr} = 2.4377 L^{0.648} \approx 0.3193t + 10.067$. He et al. (2009) have studied the relationship between U_{cr} (cm/s) and age (t, d) of juvenile Chinese sturgeon with age range 2.5–12.5 months old and obtained $U_{cr} = 0.1719t + 17.285$.

(D) The relationship between downriver migration speed and age of juvenile Chinese sturgeon. The scattered points represent three sets of velocity-age relationships by regression analysis from the data of Zhang et al. (2012) and Yang et al. (2005). The solid yellow line is the average of three sets.
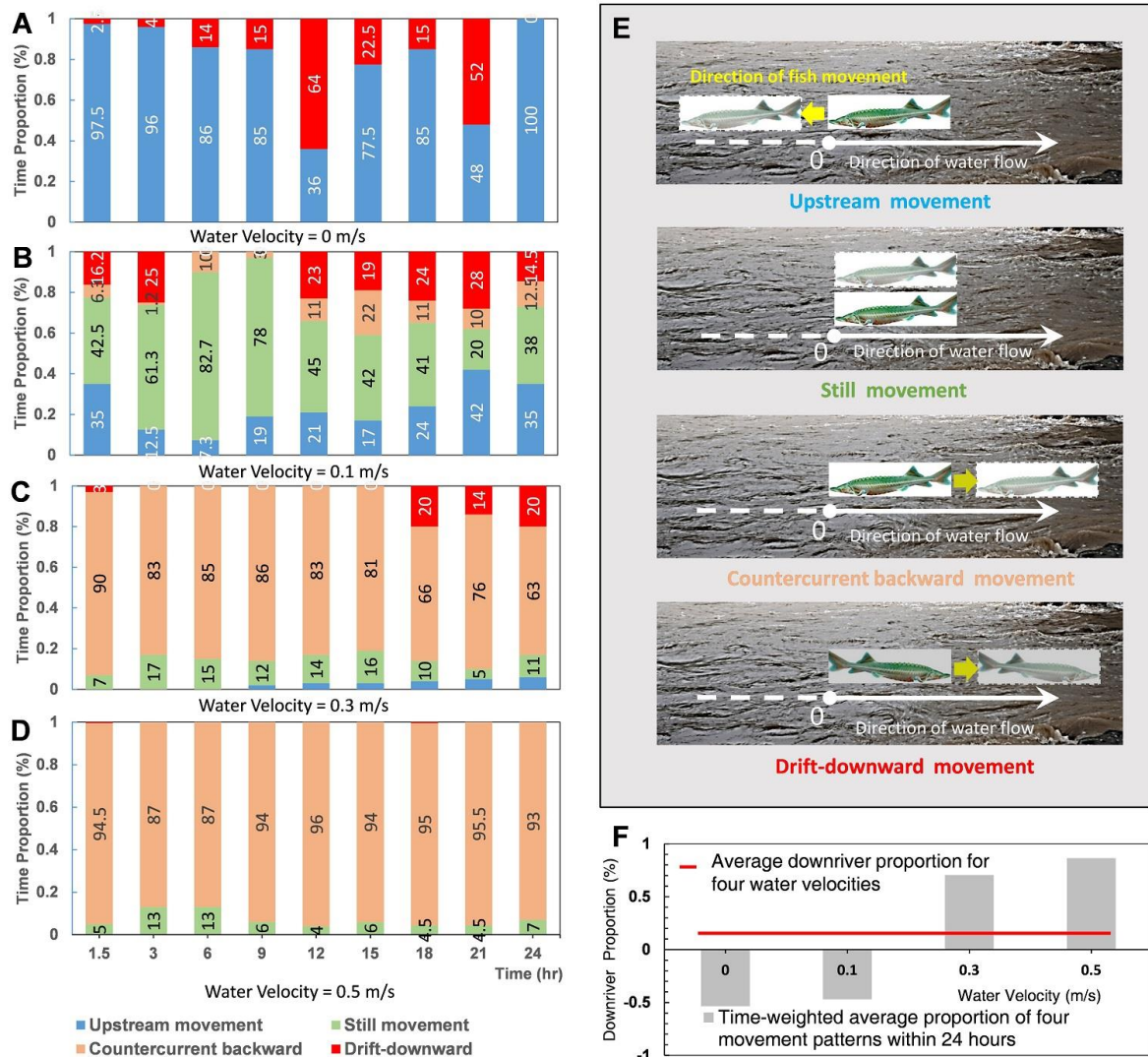
Figure S3. Effect of Water Velocity on the Time Proportion of Swimming Behavior for Juvenile Hybrid Sturgeon within 24 hours, Related to Figures 2 and 4.

(A) At a water flow velocity of 0 m/s (still water), only two states of upstream and drift-downward movements exist, and the upstream state accounts for 79.24% of the time (Li et al., 2011).

(B) At 0.1 m/s, four movement patterns exist; mainly still movement maintained at 20.2–80.1% of the time, followed by the upstream run at 8–42.1% of the time (Li et al., 2011).

(C) At 0.3 m/s, the countercurrent backward movement is the primary trend at 62.5–89.2%. As time goes on, the time percentage of the countercurrent backward swimming decreases slowly. However, that of drift-downward movement increases to be about 20% (Li et al., 2011).

(D) At 0.5 m/s, the countercurrent is the main force, accounting for 92.2–95.4%, without upstream movement (Li et al., 2011).

(E) Four movement patterns of juvenile fish involve, from top to bottom, the upstream, still, countercurrent backward, and drift-downward movements corresponding to negative, zero, positive, and positive migration speeds over the ground, respectively, when assuming that the downstream direction is positive.

(F) The average downriver proportion for four water velocities. If the downstream direction is positive, we calculated the time-weighted average proportion of four movement patterns within 24 hours at four water velocities and then obtained the average downriver proportion for the four water velocities, showing that the juvenile fish individuals swim downward at a relatively small daily average migration speed.
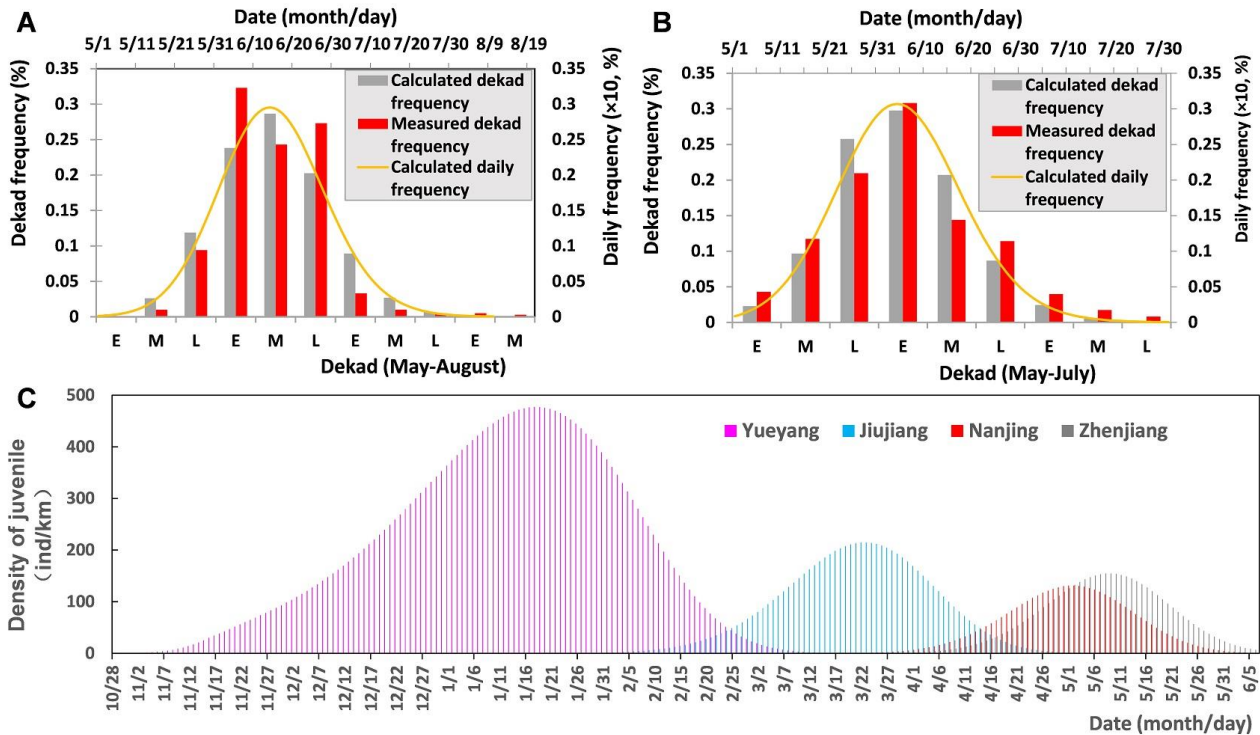
Figure S4. Comparison Between Measured and Calculated Values for Density Distributions of Juvenile Chinese Sturgeon, Related to Figures 4.

(A) Comparison between measured and calculated values for occurrence frequency of juveniles in Yangtze estuary (0 km). Yi (1994) reported the collection of juveniles as bycatch by set gillnet or other fishing gear in 1987 and between 1990 and 1992, from May to August each year in the eastern beach (Chenjia Town) of Chongming Island. Taking dekad (10-day) as a statistical unit to count the number of juveniles collected from May to August, as shown in Table S2, the term "dekad frequency" represents the occurrence frequency of juveniles every 10 days. On the abscissa (in order): E, Early; M, Middle; L, Late. In China, we usually divide each month into three periods, each period being 10 days, to represent early, mid and late month for catch statistics of juveniles.

(B) Comparison between measured and calculated values for occurrence frequency of juvenile fish at Xupu (115 km) of Changshu City. Li et al. (2011) reported the number of juveniles caught at Xupu of Changshu City between 2002 and 2009, with a range of 19–718 individuals and an average of 167 individuals, as shown in Table S2.

(C) Comparison between the calculated and observed results of the density distribution of juveniles in the four segments of the Yangtze River.

Yueyang (Chenglingji) section: Yi (1994) reported that juveniles fed and stayed for a long time in this area, which is described as appearing in January and lasting from April to May; there were no samples. The calculated results show that juvenile sturgeon in the Yueyang section appeared in early November, reached its peak in the middle and late January, and lasted until the middle of March.

Jiujiang section: Yi (1994) reported that the occurrence time of juveniles in Hukou was from January to June; the peak time was from late April to early May, and there were five individuals collected. The calculated results show that the occurrence time of juveniles in Hukou lasts from the end of January to the beginning of February, and the peak appears in late March and lasts until early May.

Nanjing section and Zhenjiang section: Yi (1994) reported that juveniles appeared with 17 individuals in samples from February to July, with the peak in May. The situation in Zhenjiang was similar to that in Nanjing, with a sample size of only one individual. The calculated results show that, due to the 72 km distance between Nanjing and Zhenjiang, the two graphs of Nanjing and Zhenjiang are overlapped. However, the calculations can still reveal the differences and details that are difficult to obtain in field investigations. The earliest occurrence time in the Nanjing section is in late March or early April, and the peak appears in early May and lasts until early June. In the Zhenjiang section, the first batch appeared in early April, and the peak in mid-May and lasts until the middle of June. Therefore, the earliest time, the peak time, and the duration of juveniles in Zhenjiang section are about one week later than those in Nanjing. Also, the migration speed of juveniles decreases, and an aggregation effect occurs after their arrival in Nanjing and entrance to the tidal-affected region.

Table S1. The Duration and Speed of Juvenile Chinese Sturgeon from Spawning Ground to the Mouth of the Yangtze River between 1996 and 2007, Related to Figures 2 and 4. (Zhang et al., 2012)

Year	Spawning Time [a]	Peak Time in Estuary Next Year	Migration Time [b] (d)	Migration Speed (km/d)
1996	20 October	Later May	218	7.68
1997	22 October	Early June	227	7.38
1998	26 October	Middle May	202	8.29
1999	27 October	Later June	243	6.89
2000	15 October	Later May	223	7.51
2001	20 October	Early June	229	7.31
2002	27 October	Later May	211	7.94
2003	6 November	Middle May	192	8.72
2004	12 November	Middle June	216	7.75
2005	10 November	Middle June	218	7.68
2006	13 November	Later May	194	8.63
Average			216	7.80

Note: [a] indicates the spawning date of first batch breeding activity; [b] indicates that the migration time was calculated in the early, middle and late 10-days of each month on the 5th, 15th, and 25th.

Ref.	Year	May			June			July			August		Total (ind)
		Early	Middle	Later	Early	Middle	Later	Early	Middle	Later	Early	Middle	
Yi, 1994	1987	1	21	98	411	180	300	67	35	10	27	11	1182
	1990	0	0	34	418	289	114	68	3	0	0	0	1127
	1991	0	l2	110	207	417	728	0	1	2	2	0	1480
	1992	0	12	166	383	177	48	11	6	6	6	0	807
	Dekad Aver.	0	11	102	352	265	298	36	11	5	5	3	1088
	Dekad Prop.	0.001	0.01	0.094	0.323	0.243	0.273	0.033	0.01	0.004	0.005	0.003	100%
Li L.X. et al., 2011	2002	ND [a]	30	36	181	12	6	4	0	0	NA [b]	NA	269
	2003	41	72	188	183	102	89	27	9	7	NA	NA	718
	2004	2	38	23	24	21	15	8	11	0	NA	NA	142
	2005	0	2	6	3	16	11	4	2	4	NA	NA	48
	2006	7	7	10	5	30	7	1	0	0	NA	NA	67
	2007	0	4	5	1	0	4	5	0	0	NA	NA	19
	2008	0	1	11	7	9	15	0	1	0	NA	NA	44
	2009	0	2	0	6	2	5	4	0	0	NA	NA	19
	Dekad Aver.	7.14	19.5	34.88	51.25	24	19	6.63	2.88	1.38	NA	NA	166.64
	Dekad Prop.	0.043	0.117	0.209	0.308	0.144	0.114	0.04	0.017	0.008	NA	NA	100%

Note: [a] ND= no data; [b] NA= not available.

Table S3. Spawning Time of Adult Chinese Sturgeon and the Starting Time of Juvenile Self-migration, Related to Figures 4.

Site	Sampling Year	Spawning Time (year-month-day)	Incubation Period [a]	Self-migration Starting Time (year-month-day)
East Beach of Chongming Island, Shanghai (Chang, 1999)	1987	1986-10-21 (1st batch) 1986-10-23 (2nd batch)	1986-10-26 1986-10-28	1986-11-13 1986-11-15
	1990	1989-10-27	1989-11-1	1989-11-19
	1991	1990-10-15 (1st batch) 1990-10-31 (2nd batch)	1990-10-20 1990-11-5	1990-11-7 1990-12-23
	1992	1991-10-23	1991-10-28	1991-1-15
	1987–1992 Aver.	22 October (1st batch) 27 October (2nd batch)	10-27 11-1	11-14 11-19
Xupu of Changshu City, Jiangsu Province (Li L.X. et al., 2011)	2002	2001-10-20 (1st batch) 2001-11-8 (2nd batch)	2001-10-25 2001-11-13	2001-11-12 2001-12-1
	2003	2002-10-27 (1st batch) 2002-11-9 (2nd batch)	2002-11-1 2002-11-14	2002-11-19 2002-12-1
	2004	2003-11-6	2003-11-11	2003-11-29
	2005	2004-11-12	2004-11-17	2004-12-5
	2006	2005-11-10	2005-11-15	2005-12-3
	2007	2006-11-13	2006-11-18	2006-12-6
	2008	2007-11-23	2007-11-28	2007-12-16
	2009	2008-11-26	2008-12-1	2008-12-19
	2002–2009 Aver.	10-31	11-5	11-23

[a] Calculated over five days of the hatchling period.

TRANSPARENT METHODS

Migration Dynamics Model (MDM) of Juveniles

Huang and Wang (2018) derived a non-linear advection-diffusion equation to obtain the spatiotemporal density distribution of the fish in the river, treating the fish as active organisms rather than as passive bodies. When considering the mortality of fish along the path, the model becomes:

$$\frac{\partial C}{\partial t} = \frac{\partial}{\partial x}\left(D\frac{\partial C}{\partial x}\right) - U\frac{\partial C}{\partial x} - KC, \tag{1}$$

where $C(x, t)$ is the density distribution or the occurrence possibility of fish, ind/km (individual per river kilometer); x is the migration distance along the river, with the Yangtze mouth (Shanghai) as the origin, km (river kilometer); t is the migration time, d (days); D is the diffusion coefficient of fish, km²/d; U is migration upriver or downriver speed of fish over the ground, depending on the active swimming ability and being associated with current, km/d; K is the instantaneous total mortality rate of the fish, which is a measure of the rate of loss of fish number in a population per day (1/d). The diffusive item, $\frac{\partial}{\partial x}\left(D\frac{\partial C}{\partial x}\right)$, expresses the random walk of the individual. The convective item, $\frac{\partial(UC)}{\partial x}$, expresses the migratory deterministic movement of the fish cohort.

Migration Stage Division and Model Parameters

Drift stage (0–8 dph)

This stage is in the downstream area of the spawning ground. The drift velocity of the larvae depends on the spatial position of the river cross-section. When they drift longitudinally with the current, the larvae move horizontally to shallow waters near the shore through a weak swing due to their phototaxis. The larvae prefer shallow water for survival and future feeding. Hence, the riverbank has a significant effect on the speed of larval movement.

Drift speed U_1 of the early larva. The drift velocity of the larvae depends on the spatial position of the river cross-section. In order to simplify the calculation, here we assume the Yangtze River as an open channel, and the exponent distribution of turbulent flow velocity in the open channel (Lu, 1990) is:

$$u = u_m\left(1 - \frac{y}{H}\right)^{1/m}, \tag{2}$$

where u is the flow velocity of cross-section of the Yangtze River and u_m the surface flow velocity; y / H is the relative water depth, where y is the water depth in a specific position and H is maximum water depth of open channel; m is a dimensionless coefficient related to the flow rate and the position of the vertical line. Yao et al. (2005) studied the cross-sectional velocity distribution at Huanglingmiao Hydrologic Station in Yichang City and found $m = 12$ for the thalweg and $m = 6$ near the bank; thus $m = 7$ is used to simplify matters in this study.

We apply the perched water layer of relative depth value y/H, obtained in the laboratory (Zhuang, 2009; Zhuang et al., 2002), to the Yangtze River. This method has been supported by Kynard et al. (2007) and Braaten et al. (2008), whereby the vertical distributions of larval pallid sturgeon in laboratory and field experiments show similar characters.

When they drift longitudinally with the current, the larvae move horizontally to shallow waters near the shores through a weak swing due to their phototaxis. Hence, the riverbank has a significant effect on the speed of larval movement. Therefore, the dimensionless shoreline influence coefficient (φ) is used,

$$\varphi = 1 - \frac{t}{8}, \tag{3}$$

where t is the age of the larva, dph.

Therefore, the drift velocity U_1 of the larvae can be modified as follows:

$$U_1 = u\varphi^2 = u_m \left(1 - \frac{y}{H}\right)^{1/7} \left(1 - \frac{t}{8}\right)^2. \tag{4}$$

Eq. 4 indicates that the larvae drift with current at the thalweg of the river at $t = 0$ dph; when $t = 1\text{-}7$ dph, the larvae move towards the shores simultaneously. This results in the decrease of drift velocity, and the larvae reach the bottom of the river where the drift velocity approaches zero at $t = 8$ dph.

The annual average velocity of Zhutuo Hydrological Station in the upper reaches of the Yangtze River is 1.61 m/s (Huang et al., 2006); the maximum velocity in Eq.4 is then $u_m = 1.61$ m/s $= 139$ km/d for pre-GD. According to the average annual velocity of typical hydrological stations in the middle and lower reaches of the Yangtze River (Yu & Zhang, 1995), we use $u_m = 1.16$ m/s $= 100$ km/d for post-GD.

Diffusion coefficient (D_1) of the early larvae. In the drift stage, the diffusion coefficient of larvae is mainly affected by the inhomogeneity of the current speed, which near the shores is much higher than that at the thalweg. Therefore, the longitudinal mixing coefficient of the river can be used to represent the diffusion coefficient of the larvae (Fisher et al., 1979; Zhao, 1986). When the larvae drift with the current and move to the shores through their weak swimming ability, the shoreline influence coefficient is used to reflect the augmentation effect of the shores on the diffusion coefficient and yields

$$D_1 = E/\varphi, \tag{5}$$

where E is the longitudinal mixing coefficient of the current, $= 5.93\ Hu_*$, where H is the water depth of the open channel and u_*, the friction velocity; φ is the shoreline influence coefficient. The longitudinal mixing coefficient (E) is the sum of the turbulent diffusion coefficient caused by turbulence and the longitudinal dispersion coefficient caused by uneven velocity distribution. The turbulent diffusion coefficient is much smaller than the longitudinal dispersion coefficient and can be neglected. Then the average longitudinal dispersion coefficient in the Three Gorges reach is used as the representative value of the main stem of the Yangtze River (Huang et al., 2006) and yields

$$E = 368\ \text{m}^2/\text{s} = 31.8\ \text{km}^2/\text{d}. \tag{6}$$

The diffusion coefficient (D_1) of larvae can be calculated by Eqs. 3, 5 and 6, as shown in Table 1.

Cover stage (9-18 dph)

Zhuang et al. (1999; 2002) reported that the early larvae begin to hide in the cracks of gravel-cobble at 8 dph and get to the peak of the individual number at 8-10 dph. The probability of hiding at 11 dph starts to decrease until 18 dph when most of the larvae leave the cracks. The larvae hide in cracks at the riverbed from 9–18 dph in the lower reaches of the spawning ground but show obvious diffusion behavior due to the local eddies. Therefore, the time-averaged velocity of current (U_2) = 0 and the diffusion coefficient $D_2 = 254.4$ km^2/d (Table 1).

Self-migration stage (after 18 dph)

Due to the limitation of observation techniques, the spatiotemporal distribution of migration velocity (U_3) of juveniles after 18 dph in the Yangtze River was difficult to obtain in the field and is related to the swimming speed and the current speed. Theoretically, the swimming speed of fish is related to body conditions such as health, body length, tail length, and swing frequency as well as environmental conditions such as water temperature, velocity, and the velocity gradient of the current. Here, we use the fishing data and mark-recapture data to estimate the model parameters.

Downriver migration speed U_3 of juveniles. (1) Estimation with fishing data. Historically, fishers used set gillnets to catch juvenile Chinese sturgeon as bycatch in the Yangtze estuary. Later, that method became a routine investigation method for the resource monitoring of the juveniles (Li L.X. et al., 2011; Zhuang et al., 2016). Zhang et al. (2012) sorted out the migration time, and interval swimming speed of juveniles from the spawning ground to

the Yangtze estuary between 1996 and 2006, as shown in Table S1. The mean migration time estimated was 216 days from the first spawning to the peak of juveniles appearing at Xupu in the following year, without deducting the incubation period of about five days. In this paper, the age of juveniles is calculated from the day of hatching (dph); the mean migration time is changed from 216 days to 211 dph, and mean migration speed is increased from 7.8 km/d to 7.99 km/d. Assuming that the self-migration started at 18 dph and the $U(t)$ of juveniles in the Yangtze River is linear with the age (t), $U(t) = at$ where a is constant, we have:

$$\frac{1}{193}\int_{18}^{18+193} U(t)dt = 7.99 \tag{7}$$

As a result, we have $a = 0.06978$. Then, the relationship between migration speed $U(t)$ and age t of the juveniles is expressed as follows:

$$U(t) = 0.06978\,t. \tag{8}$$

(2) Estimation with mark-recapture data. Yang et al. (2005) reported that 175,200 two-month-old juvenile Chinese sturgeons were released at Yichang and Shashi from 1998 to 2002, 77,957 of which were labeled with CWT; 400 fourteen-month-old juveniles were labeled with silver tags and CWT. Sample collection was carried out along the Yangtze River and the coastal waters after the release. In four years, the total catch was 6,400 of the two-month-olds and 13 of the fourteen-month-olds, among which the marked juveniles comprised 13 of the two-month-olds and 13 of the fourteen-month-olds. We can obtain the linear relationship between mean interval velocity and age.

The recapture records in 2000 showed that the two-month-old juveniles released on December 28 reached Xupu between May and July (June 15 was the median), and their migration speed was 8.5–11.3 km/d with an average of 9.8 km/d. Calculated monthly for 30 days, therefore, the release age of juveniles is 60 days (2 months old), and the age of recapture is 227 dph. The fourteen-month-old juvenile Chinese sturgeon (420 days) were released with an average migration time of 70 days and an average speed of 28.6 km/d. Therefore, we have

$$\begin{cases} \frac{1}{167}\int_{60}^{60+167} U(t)dt = 9.8 \\ \frac{1}{70}\int_{420}^{420+70} U(t)dt = 28.6 \end{cases}. \tag{9}$$

Therefore, the relationship between $U(t)$ and age t of juveniles can be expressed as follows:

$$\begin{cases} U(t) = 0.06829t, \text{ for } 2 - \text{month} - \text{old juveniles released} \\ U(t) = 0.06286t, \text{ for } 14 - \text{month} - \text{old juveniles released}' \end{cases} \tag{10}$$

where $U(t)$ is the migration speed of the juveniles, km/d; t is the age of fish, dph.

We used the fishing and mark-recapture data to obtain similar expressions for the speed function and took the average value of Eqs. 8 and 10 as the migration speed of juveniles.

$$U_3 = 0.06698\,t \tag{11}$$

After the juveniles enter the tidal-affected region, the current is slowed down by the tide, resulting in a corresponding decrease of the migration speed of juveniles. The tag-tracking measurements in 2015–2016 showed that the migration speed of 3.5-year-old subadults after entering Nanjing was reduced by about 20% (Institute of Chinese Sturgeon of China Three Gorges Corporation, Preliminary report on the tag-tracking experiment of cultured Chinese sturgeon in 2015–2016, internal report). Therefore, the reduction of current speed has a more significant impact on the migration speed of juveniles. In this paper, we assume that the migration speed of juveniles from Nanjing to the estuary is reduced by 30% and introduce a tidal influence coefficient (γ) into Eq. 11 in the tidal-affected region. Then, we have

$$U_3 = 0.06698\,t\,\gamma \tag{12}$$

where γ is the tidal influence coefficient, $\gamma = 0.3\frac{x}{\Delta L} + 0.7$, as $x \leq 347$ km; $\gamma=1$, as $x > 347$ km (above Nanjing); $\Delta L = 347$ km, the distance between Nanjing and the estuary.

It should be noted that the migration speed equation (Eq. 12), recommended in this paper, represents the combined effects of the juveniles' swimming ability and the current speed, and reflects the common trait of downriver migration speed at large spatiotemporal scale and the population level. However, rich detail of the migration speed still lacks at a smaller spatiotemporal scale and at the individual level.

Diffusion coefficient (D_3) of juveniles. In the self-migration stage, D_3 is synthetically determined by the swimming ability and the current speed; of the two, the current effect on the juvenile migration speed decreases with age. Therefore, we divide D_3 into two parts: the fish-related diffusivity (D_f), which is determined by the juvenile swimming ability increasing with age, and the current-related diffusivity (D_w), which is determined by the current speed and is attenuated with the increase in age.

(1) Estimation of D_f. Based on the random walk theory, the fish-related diffusivity D_f can be expressed as follows (Zhao, 1986):

$$D_f = \frac{V*dx}{2}, \tag{13}$$

where V is the random walk velocity of the individual; and dx is the walk distance of each step of the individual.

We introduce the Peclet number as follows (Fisher et al., 1979; Zhao, 1986):

$$P_e = \frac{U*l}{D_f}, \tag{14}$$

where the dimensionless Peclet number, P_e, denotes the ratio of convection item to diffusion item; U is the characteristic velocity, and l is the characteristic length.

Assuming the random walk velocity (V) and the characteristic velocity (U) of individual are expressed by the migration speed of juveniles, $U(t)$, then $V = U = U(t)$, while the walk distance dx of each step and the characteristic length l can be expressed by the full length (L) of juveniles, namely $dx = bL$ (b is constant) and $l = L$; then Eqs. 13 and 14 become

$$D_f = \frac{b}{2}U(t)L \tag{15}$$

$$P_e = \frac{U(t) \times L}{D_f} = constant \tag{16}$$

Substituting the linear regression relationship of full length–age (Figure S2B) and Eq. 11 into Eq. 15, we have

$$D_f = 4.2 \times 10^{-3}bt^2 + 4.8 \times 10^{-2}bt \tag{17}$$

Using the diffusion coefficient obtained by the tag-tracking experiment of 3.5-year-old sub-adults (Huang & Wang, 2018), $t = 3.5$ a $=1277.5$ d and $D_f =1550$ km^2/d, meanwhile assuming that the diffusion coefficient of 3.5-year-old subadult is less affected by current, then we have $b = 0.2238$ from Eq. 17. Thus, Eqs. 15 and 16 become

$$\begin{cases} D_f = 9.414 \times 10^{-4}t^2 + 1.075 \times 10^{-2}t \\ P_e = 8.94 \end{cases} \tag{18}$$

Eq.18 shows that the fish-related diffusivity D_f is proportional to age (t) squared and the convective term is predominant, about nine times the fish-related diffusivity term in the migration process of juveniles.

(2) Estimation of D_w. In the drift stage, we have calculated that the diffusion coefficient of 7-dph larvae is 254.4 km²/d and is also used in succession in the cover stage (8-18 dph). In the self-migration stage, the effect of water flow on swimming attributes weakens with age. Therefore, we assume that the current-related diffusivity (D_w) will decrease with the age of the juvenile. So, we can construct a function of (D_w) as follows:

$$D_w = \frac{254.4}{\sqrt{t-18}} \qquad (19)$$

The diffusion coefficient of juvenile D_3 in the self-migration stage ($t > 18$ dph) was obtained as follows:

$$D_3 = D_f + D_w = 9.414 \times 10^{-4} t^2 + 1.075 \times 10^{-2} t + \frac{254.4}{\sqrt{t-18}}, \qquad (20)$$

where t is the age of the juvenile, dph.

The Mortality Rate of Young Chinese Sturgeon

In the early life stage of lake sturgeon, the larval mortality rate is more than 99.9%, which has a significant impact on the recovery of the population size (Caroffino et al., 2008; 2010). Similar to the lake sturgeon, the mortality of the juvenile Chinese sturgeon during the migration process in the Yangtze River also significantly affects their future population size.

The eggs are rapidly fertilized while depositing onto the riverbed of spawning ground and adhering to the cracks of the gravel-cobble substrate. Fertilized egg survival depends on egg predation and the fertilization rate during the sinking process. Wei (2003) reported that the fertilization rate of wild Chinese sturgeon from 2000 to 2002 was 79.3–93.4%, with an average of 86.4%. Ke et al. (1989) reported three field tests of Chinese sturgeon egg release carried out at 5:00 pm, involving 400,000 unfertilized eggs sprinkled on the spawning ground downstream from the GD for the first and the second tests; the third field test involved 800,000 fertilized eggs sprinkled at the same place a few days later. Each time predators such as *Coreius guichenoti*, *Coreius heterodon,* and *Pelteobagrus vachelli* were captured, they were dissected the next day. The test results showed that the average mortality rate was 84% for eggs swallowed by the predators during the sinking process on the day of spawning. Therefore, the survival rate of 0-day fertilized eggs was 13.8% = (1−84%) ×86.4%, as shown in Figure 3.

Fertilized eggs adhered to the bottom pebbles for five days to hatch out into early larvae. The hatching rate of fertilized eggs was 70% (Chang, 1999), and the threats to eggs come mainly from predatory egg fish. Chang (1999) reported a regression function of the occurrence percentage of benthonic predators that appeared day-by-day after spawning, so that the function reflected the density-dependent probability of developing eggs being devoured by predators (Justice et al., 2009). If considering the mortality rate of 0-day fertilized eggs to be 84%, we can obtain the mortality rate of larvae day by day as follows:

$$K_0 = 0.84 \, e^{-0.2867T}, \qquad (21)$$

where K_0 is the mortality rate caused by egg predation and decreases with time. Mortality by predation mainly occurs in the drift stage and the early self-migration stage; T is the number of days after spawning, d. A similar result to Eq. 21 was reported for eggs of lake sturgeon (Caroffino et al., 2010). Therefore, the cumulative mortality rate by predators at the end of the cover stage (18-day) is estimated to be 96%, so the survival rate from 1-day fertilized eggs to late larvae is 2.8% = (1−96%) × 70%.

When entering the self-migration stage (18 dph), juveniles begin to feed, and their swimming ability has gradually enhanced. The total mortality rate of juveniles includes both natural and anthropogenic mortality sources, mainly due to starvation (Caroffino et al., 2008), water pollution (Hu et al., 2009), bycatch (Chang, 1999) and a variety of hydrological conditions, including the effects of saltwater in the estuary (He et al., 2009; Zhao, Qu & Zhuang et al., 2011; Zhao, Zhuang & Zhang et al., 2015); however, the threat of predators decreases with the age and growth of larvae (Ke et al., 1989). To estimate the amount of juvenile Chinese sturgeon with mark-recapture tests, Wei (2003) used a mortality rate of 90% from the release site in the spawning ground to the recapture site in the estuary, 50%

of which occurred during a stay in the estuary. Therefore, we take the mortality of juveniles as 90% during the self-migration stage from the hatching site to the estuary, evenly distributed with time along the river reach, and 50% during the next stay in the estuary. We have:

$$K = \frac{2.3}{T}, \tag{22}$$

where K is an instantaneous total mortality rate in Eq.1, 1/d; T is the number of days when a juvenile spends from the hatching site to the estuary, d. We can estimate $T = 288$ d for pre-GD and $T = 228$ d for post-GD from the migration speed of the fish, including U_1, U_2, and U_3 mentioned above.

Numerical Method of MDM

Our MDM is nonlinear and has variable coefficients. It requires a large calculation space, long calculation time, and high conservation of number when numerical methods are used. MATLAB software was used for discretization calculation of the MDM. Due to the existence of the convection item, the convection-diffusion equation often displays numerical instability and oscillations. After a comparison of methods and schemes, we selected the Crank–Nicolson scheme of finite difference methods for a discretization calculation to obtain numerical results. The scheme is unconditionally stable (Crank & Nicolson, 1996). The discretization form is:

$$\frac{C_j^{i+1}-C_j^i}{\Delta t} = \frac{1}{2}\left[\frac{\left(C_{j+1}^{i+1}+C_{j-1}^{i+1}-2C_j^{i+1}\right)D^{i+1}}{\Delta x^2} + \frac{\left(C_{j+1}^i+C_{j-1}^i-2C_j^i\right)D^i}{\Delta x^2}\right] - \frac{1}{2}\left[\frac{(UC)_{j+1}^{i+1}-(UC)_{j-1}^{i+1}}{2\Delta x} + \frac{(UC)_{j+1}^i-(UC)_{j-1}^i}{2\Delta x}\right] - KC_j^i, \tag{23}$$

where Δx and Δt are spatial and temporal steps, respectively; the superscript of C represents the time node, and the subscript represents the space node. The rearranged equation is:

$$\left(-\frac{U_{j-1}^{i+1}}{4\Delta x} - \frac{D^{i+1}}{2\Delta x^2}\right)C_{j-1}^{i+1} + \left(\frac{1}{\Delta t} + \frac{D^{i+1}}{\Delta x^2}\right)C_j^{i+1} + \left(\frac{U_{j+1}^{i+1}}{4\Delta x} - \frac{D^{i+1}}{2\Delta x^2}\right)C_{j+1}^{i+1} =$$

$$\left(\frac{D^i}{2\Delta x^2} + \frac{U_{j-1}^i}{4\Delta x}\right)C_{j-1}^i + \left(\frac{1}{\Delta t} - \frac{D^i}{\Delta x^2} - K\right)C_j^i + \left(\frac{D^i}{2\Delta x^2} - \frac{U_{j+1}^i}{4\Delta x}\right)C_{j+1}^i, \tag{24}$$

where $C_{j-1}^{i+1}, C_j^{i+1}, C_{j+1}^{i+1}$ are unknown items to be solved at time $i+1$; all on the right side are known items at time i.

If the maximum time length that a distributed cohort spends from the hatching area to the river mouth is T_M, and the numbers of space nodes (m) and time nodes (n) are:

$$\begin{cases} m = \frac{L}{\Delta x} + 1 \\ n = \frac{T_M}{\Delta t} + 1 \end{cases} \tag{25}$$

Therefore, the linear equation set in the calculation is:

$$\begin{pmatrix} \beta_1 & \alpha & \gamma_3 & 0 & 0 \\ \cdots & \cdots & \cdots & \cdots & \cdots \\ 0 & \beta_{j-1} & \alpha & \gamma_{j+1} & 0 \\ \vdots & \vdots & \vdots & \vdots & \vdots \\ 0 & 0 & 0 & \beta_{m-2}+\gamma_m & \alpha \end{pmatrix} \begin{pmatrix} C_1^{i+1} \\ \vdots \\ C_j^{i+1} \\ \vdots \\ C_{m-1}^{i+1} \end{pmatrix} = \begin{pmatrix} -\beta_1'C_1^i + \alpha'C_2^i - \gamma_3'C_3^i \\ \vdots \\ -\beta_{j-1}'C_{j-1}^i + \alpha'C_j^i - \gamma_{j+1}'C_{j+1}^i \\ \vdots \\ -(\beta_{m-2}'+\gamma_m')C_{m-2}^i + \alpha'C_{m-1}^i \end{pmatrix}, \tag{26}$$

where $\alpha = \frac{1}{\Delta t} + \frac{D^{i+1}}{\Delta x^2}$; $\beta_{j-1} = -\frac{U_{j-1}}{4\Delta x} - \frac{D^{i+1}}{2\Delta x^2}$; $\gamma_{j+1} = \frac{U_{j+1}}{4\Delta x} - \frac{D^{i+1}}{2\Delta x^2}$; $\alpha' = \frac{1}{\Delta t} - \frac{D^i}{\Delta x^2} - K$; $\beta_{j-1}' = -\frac{U_{j-1}}{4\Delta x} - \frac{D^i}{2\Delta x^2}$; $\gamma_{j+1}' = \frac{U_{j+1}}{4\Delta x} - \frac{D^i}{2\Delta x^2}$

The linear equations set (Eq.26) can be expressed by $\mathbf{AC} = \mathbf{B}$. $\mathbf{A}$ is a matrix of m rows and n columns, $\mathbf{B}$ is a matrix of m rows and one column, and $\mathbf{C}$ is a matrix of m rows and one column. The matrixes are as follows:

$$A = \begin{pmatrix} \beta_1 & \alpha & \gamma_3 & 0 & 0 \\ \cdots & \cdots & \cdots & \cdots & \cdots \\ 0 & \beta_{j-1} & \alpha & \gamma_{j+1} & 0 \\ \vdots & \vdots & \vdots & \vdots & \vdots \\ 0 & 0 & 0 & \beta_{m-2}+\gamma_m & \alpha \end{pmatrix} \tag{27}$$

$$B = \begin{pmatrix} -\beta_1' C_1^i + \alpha' C_2^i - \gamma_3' C_3^i \\ \vdots \\ -\beta_{j-1}' C_{j-1}^i + \alpha' C_j^i - \gamma_{j+1}' C_{j+1}^i \\ \vdots \\ -(\beta_{m-2}' + \gamma_m') C_{m-2}^i + \alpha' C_{m-1}^i \end{pmatrix} \tag{28}$$

$$C = \begin{pmatrix} C_1^{i+1} \\ \vdots \\ C_j^{i+1} \\ \vdots \\ C_{m-1}^{i+1} \end{pmatrix} \tag{29}$$

The Matlab software platform provides various calculation methods for the linear equation set, $\mathbf{AC} = \mathbf{B}$, such as the left division ($\mathbf{C} = \mathbf{A} \backslash \mathbf{B}$) and inversion method ($\mathbf{C} = \text{inv}(\mathbf{A}) \times \mathbf{B}$). The inversion method requires that $\mathbf{A}$ is a square matrix. Therefore, we use the left division method in this study.

The density distributions of juveniles in the downriver migration process can be calculated based on the above methods and procedures.

Initial and boundary conditions in the calculation

The spawning activity of Chinese sturgeon was affected by the gonadal development and environment, but with a small change of the spawning time for pre-GD and post-GD. The activity was mainly due to the environmental change caused by the transfer of the spawning ground from upstream to 1,000 km downstream, so that the spawning time was delayed from mid-October to late-October. The incubation period of eggs was 5 days, which has remained unchanged.

In pre-GD, the first spawning time was October 20 on average (YARSG, 1988), and the spawners participating in breeding accounted for 70% of the population size (Huang & Wang, 2018). The first batch of eggs hatched on October 25, which was counted as 0 dph. On November 12, the larva reached the age of 18 dph and entered the self-migration stage. The second spawning time was five days later (October 25), and the remaining 30% of the population size finished breeding and entered the self-migration stage on November 17.

In post-GD, the dam had effects on the spawning activities of Chinese sturgeon, resulting in a delay of spawning time. We adopt that the average spawning time was October 27, so that larvae hatched on November 1 for the age of 0 dph and reached 18 dph on November 19, entering the self-migration stage.

The number of early larvae (18 dph) for pre-GD was $N = 780,000$ individuals. For post-GD, $N = 185,000$ individuals.

Calculated river length: $L = 2,850$ km for pre-GD; $L = 1,675$ km for post-GD.

Initial larval distribution: uniform within the typical spawning site such as Sankuaishi of pre-GD and Huyatan of post-GD at $\Delta L = 30$ km.

Model Verification

Li (2014) reported that cultured juveniles had formed a saltwater adaptation mechanism after 5 months of age. Zhao et al. (1986) observed that the earliest juvenile fish appeared in the estuary from 1982 to 1985 was early May, which is consistent with the results of this paper. The data of year-long investigation in the estuary by Yi (1994) (Figure S4A) and Li L.X. et al. (2011) (Figure S4B) showed that the peak time of juveniles occurred in mid-June, which is consistent with the calculated results in Figure 4B. Chen et al. (2016) analyzed the occurrence time in the Yangtze estuary from 2005 to 2013 and concluded that in most years, the earliest occurrence time was concentrated in the period of May to mid-June, and the final departure time was from mid-July to late-August; the average occurrence time lasted 82 days (about 2.7 months). These survey findings are very similar to the calculated results in this paper.

We used the dekad (10-day) data from Yi (1994) and Li L.X. et al. (2011) to verify the theoretical model. Because of the small number of samples collected each year relative to the fecundity of the fish, we used the average values of the sampling data of 1987–1992 and 2002–2009 to eliminate the random error caused by the small sample size. The initial conditions of the calculations for 1987–1992 and 2002–2009 are shown in Table S3; these include the spawning time, incubation period and self-migration starting time. We used the average values listed in Table S3 in the calculations. Therefore, we compared the fishing data with the calculated results to verify the rationality and reliability of the model.

East Beach data (1987–1992) of Chongming Island

Quantitative verification: Figure S4A shows the comparison between the measured and calculated values of the occurrence frequency of juveniles in the eastern beach of Chongming Island, which is the core zone of the National Nature Reserve of Juvenile Chinese sturgeon and is the last stop for the downriver migration of juveniles. Therefore, the eastern beach of Chongming is an ideal site for population surveillance. The occurrence frequency of juveniles is indicated by the proportion of the collected amount per ten days to the annual collection. Hence, we processed the daily data in the calculation into dekad (10-d) data for comparison. Additionally, we multiplied the daily frequency by 10 and drew it in the same figure. The calculated results in this paper are in good agreement with the annual average data from 1987 to 1992, demonstrating the rationality of the theoretical model.

Qualitative verification: Yi (1994) reported a simple description of the juvenile occurrence downstream of the GD in places such as Yisha, Yueyang, Jiujiang, Nanjing, and Zhenjiang sections. Excluding the Yisha section located in the spawning ground, we calculated the density distributions of juveniles in Yueyang (401 km), Jiujiang (882 km), Nanjing (1,328 km), and Zhenjiang (1,402 km) sections to qualitatively verify the correctness of the model, as shown in Figure S4C. In summary, the calculated results of this paper are consistent with the recorded data (Yi, 1994), which shows the rationality of the model's calculations.

Xupu data (2002–2009) of Changshu City

The density distribution of juveniles at Xupu (1,575 km) of Changshu City was simulated. Figure S4B shows that the calculated results are in good agreement with the fishing data at Xupu from 2002 to 2009, verifying that our model is reasonable and feasible.

Data and Software Availability

Raw data for the model parameters and calculated results (Figure 4) and their Matlab software code are available online via a Mendeley Data repository with DOI links at doi:10.17632/gyg6gg4mtk.1.

Supplemental References

Caroffino, D.C., Sutton, T.M., Elliott, R.F. & Donofrio, M.C. (2008). Early life stage mortality rates of lake sturgeon in the Peshtigo River, Wisconsin. N. Am. J of Fish Manag. *30*, 295-304. Doi:10.1577/M09-082.1.

Caroffino, D.C., Sutton, T.M., Elliott, R.F. & Donofrio, M.C. (2010). Predation on early life stages of lake sturgeon in the Peshtigo River, Wisconsin. Trans. of the Am. Fish Soc. *139*, 1846-1856. Doi: 10.1577/T09-227.1.

Chen, J.H., Liu, J., Wu, J.H., Xu, J.N., Zheng, Y.P., Chen, H.W. & Dai, X.J. (2016). Analysis on the fluctuation features of recruitment for juvenile Chinese sturgeon, *Acipenser sinensis* in the Yangtze River estuary. J of Shanghai Ocean Uni. *25*(3), 381-387. Doi:10.12024/jsou. 20150901565.

Crank, J. & Nicolson, E.A. (1996). Practical method for numerical evaluation of solutions of partial differential equations of the heat-conduction type. Advances in Computational Mathematics *6*, 207-226.

Duan, M., Zhuang, P., Zhang, L.Z., Feng, G.P., Huang, H.L., Chen, S., Qu, Y. & Yan, J. (2011). Study on critical swimming speed and its morphology of juvenile Chinese sturgeon. Summary of Papers of the Annual Meeting of the Chinese Fisheries Society in 2010.

Fisher, H.B., List, E.J., Koh, R.C.Y., Imberoer, J. & Brooks, N.H. (1979). *Mixing in inland and coastal waters* (New York: Academic Press).

Huang, Z.L., Li, Y.L., Chen, Y.C., Li, J.X., Xing, Z.G., Ye, M., Li, J., Lu, P.Y., Li, C.M. & Zhou, X.Y. (2006). *Water quality prediction and water environmental carrying capacity calculation for Three Gorges Reservoir* (Beijing: China WaterPower Press).

Justice. C., Pyper, B.J., Beamesderfer, R.C.P., Paragamian, V.L., Rust, P.J., Neufeld, M.D. & Ireland, S.C. (2009). Evidence of density- and size-dependent mortality in hatchery-reared juvenile white sturgeon (*Acipenser transmontanus*) in the Kootenai River. Can. J. Fish. Aquat. Sci. *66*, 802–815. Doi:10.1139/F09-034.

Ke, F.E., Hu, D.G., Zhang, G.L., Luo, J.D., Wei, Q.W. & Zhuang, P. (1989). Investigation of ecological effect of Gezhouba Dam on the resource of Chinese sturgeon. In *Selected works of a colloquium on major technical issues of Gezhouba Dam fourth volume–fish rescue*, Gezhouba representative office of Ministry of Water Conservancy and Electric Power and Yangtze River Water Conservancy Committee eds. pp.231-254.

Kynard, B., Parker, E., Pugh, D. & Parker, T. (2007). Use of laboratory studies to develop a dispersal model for Missouri River pallid sturgeon early life intervals. J Appl. Ichthyol. *23*, 365-374.

Li, L.X., Zhang, H., Wei, Q.W., Du, H. & Hong, K.M. (2011). Occurrence time and amount variation of juvenile Chinese sturgeon, *Acipenser sinensis* at Xupu, Changshu section of Yangtze River after closure of Three Gorges Dam. J of Fishery Sciences of China *18*(3), 611-618. Doi:10.3724/SP.J.1118.2011.00611.

Li, W. (2014). Mechanisms of salinity effects on growth performance and isosmotic point calculation in anadromous fish, Chinese sturgeon (*Acipenser sinensis*). Doctoral thesis, Huazhong Agricultural University, Wuhan, China.

Lu, J.Y. (1990). Study on velocity distribution of Yangtze River flow. J of Yangtze River Sci. Res. Inst. *7*(1), 40-49.

Yao, S.M., Lu, J.Y. & Xu, H.T. (2005). Study of vertical velocity distribution at Huanglingmiao hydrologic section. J of Yangtze River Sci. Res. Inst. *22*(4), 8-11.

Yu, W.C. & Zhang, J. (1995). Analysis of resistance coefficient for lower Yangtze stretch. Yangtze River *26*(4), 8-24. Doi: 10.16232/j.cnki. 1001-4179.1995.04.003.

Zhang, H., Wei, Q.W., Li, C., Du, H., Liao, W.G. (2012). Effects of high-water level on the river residence period of juvenile Chinese sturgeon *Acipenser sinensis* in the Yangtze River. Knowl. Manag. Aquat. Ecosyst. *405*, 02p01-14. Doi: 10.1051/kmae/ 2012007.

Zhao, W.Q. (1986). *Environmental Hydraulics* (Chengdu: Chengdu University of Science and Technology Press).

Zhao, Y., Huang, L. & Yu, Z.T. (1986). Investigation of the current situation on juvenile Chinese sturgeon. Reservoir Fisheries *6*, 38-41.